ABSTRACT

ALILI, ABBAS. Wearable Robotic Solutions for Enhanced Mobility and Balance for People with Lower Limb Amputation. (Under the direction of Dr. He Huang).

Recent advancements in wearable lower-limb robotics have led to the development of devices like powered exoskeletons and prosthetics, which enhance mobility and help restore natural movement in individuals with lower-limb amputations. A key focus has been designing control systems for these devices to replicate normal joint movements and forces, improving gait performance for users. Control objectives for such devices are typically centered around three main goals: (1) gait naturalness - improving loading symmetry, spatiotemporal parameters (such as step length, time spent on each leg, gait phase duration), and joint angles during walking phases; (2) gait efficiency - aimed at reducing metabolic rate and increasing walking speed; and (3) wearable device responsiveness - emphasizing adaptability to the user's behavior and environment, especially in direct EMG control, where precision under voluntary control is essential.

While many control objectives are quantifiable and mechanically achievable, they do not fully capture the complexity of human-machine interaction. Two factors that have not been extensively researched or integrated into robotic exoskeleton and prosthesis control are user preference and gait balance. Allowing users to influence the control system based on their preferences, and incorporating those preferences into the control architecture, can lead to a more holistic understanding of user needs and guide the development of improved control systems. Feedback from clinicians and recent surveys of lower-limb amputees indicate that gait balance and stability are among the most desired features users seek access to. Unfortunately, current robotic exoskeletons and prostheses do not prioritize gait balance as a primary control objective, relying instead on users to manage it themselves.

To address this gap, this doctoral study aimed to incorporate user preferences into the control architecture of a robotic knee prosthesis. We developed a novel tuning framework featuring (1) a user-controlled interface for selecting preferred knee kinematics and (2) a reinforcement learning-based algorithm to adjust prosthesis control parameters. We evaluated the framework's performance and usability, investigating whether amputee users could identify and select preferred control profiles. Results showed that users could consistently choose their preferred knee control profile, and the framework effectively tuned 12 prosthesis control parameters to match these preferences. A blind comparison study further confirmed users' ability to differentiate between preferred and other profiles. This preference-driven framework revealed that gait balance is the top priority for prosthesis users when selecting target knee kinematics for the RL auto-tuning system.

With gait balance in mind, we developed a bilateral hip exoskeleton with admittance control to modulate step width, which is crucial for enhancing mediolateral balance during walking. This phase aimed to assess how step width responds to changes in the exoskeleton's control parameters. Results showed that step width significantly adjusted within four heel strikes following a stiffness change for non-disabled individuals, while step length and gluteus medius EMG activity remained unchanged. Additionally, we demonstrated how step width modulation influences gait balance using common gait balance metrics.

Finally, we developed a novel control framework to accurately regulate the step width of mediolaterally active robotic hip exoskeleton users. The framework utilized a reinforcement learning-based approach to adaptively tune the PID controller, accounting for the hip and exoskeleton dynamics to control step width. This control framework was tested with both non-disabled and lower-limb amputee participants, showing accurate and robust step width control.

Through this work, we advanced the field of robotic prostheses and exoskeletons by developing two distinct frameworks: one that integrates user needs into the control of robotic prostheses, and another that provides accurate and robust step width control with a robotic hip exoskeleton to enhance gait balance.

Wearable Robotic Solutions for Enhanced Mobility and Balance for People with Lower Limb Amputation

by
Abbas Alili

A dissertation submitted to the Graduate Faculty of
North Carolina State University
in partial fulfillment of the
requirements for the degree of
Doctor of Philosophy

Electrical Engineering

Raleigh, North Carolina
2024

APPROVED BY:

Dr. H Troy Nagle Jr	Dr. Edgar Lobaton
Dr. Nitin Sharma	Dr. He Huang Chair of Advisory Committee

DEDICATION

This dissertation is dedicated to my family! Dad and Mom, I love you both deeply. Your unwavering love and support have been my constant motivation throughout this journey and every journey. To my wife, Aytan, your support, kindness, and unconditional love have inspired me every step of the way. Aslan and Jacqueline, it is a gift to have you both and to feel your support. Takin and Matin, my qofiks, I love you! I love you All!

BIOGRAPHY

Abbas Alili was born in Baku, Azerbaijan, to Ilham Aliyev and Sahira Aliyeva. He earned his Bachelor's degree in Automation and IT from Azerbaijan State University of Oil and Industry in 2010, graduating with honors. He later obtained a Master’s degree in Electrical and Computer Engineering from the University of Stuttgart, Germany, in 2014. From 2014 to 2019, he was a Senior Lecturer at Baku Higher Oil School, teaching process control and microcontrollers, establishing an IoT lab, and developing CCTV analysis for oil and gas safety. In 2019, Abbas relocated to the United States to pursue his Ph.D. in Electrical and Computer Engineering at North Carolina State University. His research focuses on wearable robotics, control systems, and machine learning, under the guidance of Dr. He (Helen) Huang. Abbas’s work includes projects in robotic exoskeletons and prostheses, with applications in gait stability and human-robot interaction. Abbas has worked in both academic and industry roles, including projects with Bosch GmbH, North Carolina State University, and Kyungsung University.

ACKNOWLEDGMENTS

This dissertation would not have been possible without the support and assistance of many individuals throughout my graduate studies.

First and foremost, I extend my heartfelt gratitude to my advisor, Dr. He (Helen) Huang, for her unwavering support, encouragement, guidance, and thoughtful critiques. Her extensive knowledge and inspiring vision have greatly motivated me to pursue excellence and grow as a researcher. I am also deeply appreciative of my committee members, Dr. Troy Nagle, Dr. Edgar Lobaton, and Dr. Nitin Sharma, for their generous contributions of time, expertise, and their valuable feedback on this dissertation. Additionally, I wish to thank Dr. Jennie Si, Dr. Jesse Dean, and Dr. Jing Feng for their guidance in collaborated projects.

I am immensely grateful to all current and past lab members at the Neuromuscular Rehabilitation Engineering Laboratory (NREL) for fostering a supportive lab environment and providing valuable insights into my research. I especially thank Varun Nalam for his patience and assistance in addressing emerging challenges; I couldn't have done this without you! My gratitude also extends to Minhan Li, Joshua Tacca, Amirreza Naseri, and Aaron Fleming for their collaborative spirit and helpful discussions. I'd also like to thank Austin Mituniewicz, Brendan Driscoll, Woolim Hong, Wentao Liu, Noah Rubin, Robert Hinson, Bretta Fylstra, Joseph Berman, and John Patterson for their support. Special thanks go to Jing Yuan and Xiaolu Bai for their essential contributions to collaborative research.

To all the participants in these studies— I owe you a deep debt of gratitude for your trust, time, effort, and patience. I cherished our conversations, and the life stories you shared. It has been a pleasure to involve you in the development of innovative wearable robotics technologies, and I hope that this research will help make life easier and more fulfilling for you.

Friends who become a family: Gokhan & Shirin, Tugrul & Elif! Thanks to God that made me to meet you. I appreciate every minute, every moment spent with you!

TABLE OF CONTENTS

LIST OF TABLES

LIST OF FIGURES

CHAPTER 1

1.1 Background

1.1.1 Individuals with Lower Limb Amputation

Globally, more than 50 million individuals are affected by lower limb amputation [1], and this figure is expected to double by 2025, driven by the rising prevalence of dysvascular diseases and an aging population [2]. Losing a lower limb is a major health event that can greatly compromise a person's mobility, balance, safety, and independence. It leads to a loss of walking ability and hinders daily activities, while also posing significant psychological and social challenges.

1.1.2 Robotic Knee Prosthesis

With technological advancements, robotic lower limb prostheses are becoming increasingly accessible to amputees, offering devices capable of mimicking natural joint movements and providing active support across a variety of tasks. These prostheses have shown considerable potential in numerous areas, such as enhancing inter- and intra-joint coordination [3], reducing energy expenditure [4], improving customization [5], [6], adapting to various terrains and activities [7], and increasing resilience to disturbances [8].

Recent research efforts have centered on refining the mechanical design of powered prosthetic limbs, with a focus on improving active force generation and transmission. Noteworthy contributions in this area include works by Lenzi et al. (2018), Liu et al. (2012), and Azocar et al. (2020) [9]–[11].

A widely used approach in prosthetic devices is the finite state machine impedance controller (FSM-IC) [12], [13]. Research suggests that the human nervous system adjusts the impedance of lower limb joints to maintain stable and robust movement across different terrains

[14], [15]. During locomotion, the gait cycle is divided into distinct phases, or states, of the finite state machine. Engineers define the rules for transitioning between these states based on specific criteria or sensor data, such as ground reaction forces or joint kinematics/kinetics. The FSM-IC framework modulates prosthetic joints to achieve desired mechanics—whether in torque, position, or impedance—according to the gait phase. These controllers are often equipped with multiple locomotion modes to accommodate varying environments, such as stair and ramp ascent/descent, or level-ground walking. Ongoing research is exploring ways to enhance these control methods by integrating learning-based techniques and adaptive algorithms, aiming to better tailor prosthetic assistance to individual users and improve their overall experience. This push for advanced control systems seeks to align mechanical capabilities more closely with user needs, leading to more intuitive and effective prosthetic solutions [16].

1.1.3 Robotic Exoskeletons

Powered lower-limb orthotic devices, or powered exoskeletons, are widely used in rehabilitation and gait assistance. Significant research has focused on enhancing their performance, particularly addressing the challenges of portability and safe user-environment interaction, with control being a key factor [17].

There are two main types of exoskeletons for gait assistance: full mobilization and partial assistance. Full mobilization exoskeletons, such as the ReWalk [18], are designed for individuals with severe motor impairments, like spinal cord injuries. These devices generate all the necessary movement torque and use simple position control, as they don't need to coordinate with voluntary leg movements. Gait initiation is often triggered by upper body movements or buttons, dramatically improving mobility for users with no independent gait.

Partial assistance exoskeletons, which are lighter, cater to individuals with less severe impairments, such as those caused by aging, lower limb amputation, incomplete spinal cord injuries, stroke, or neurodegenerative diseases. These devices also support healthy users by enhancing endurance but require more sophisticated control due to the complex interaction with the user. While their end goals differ, both rehabilitation and mobility-assistance devices share many control techniques.

1.1.4 Preference Based Control and Gait Balance Improvement

Research over the past decades has focused on improving the mechatronic design and control of wearable devices, resulting in lightweight, powerful, and untethered systems [19]. However, a universal set of objectives for guiding the design, control, and assessment of wearable robotics remains elusive. Key design and control decisions, such as tuning control parameters or selecting design features like mechanical stiffness, are critical for achieving desired biomechanical or physiological effects. Metrics such as symmetry [20], range of motion [21], muscle activation [22], joint loading [4], and metabolic rate [23] have commonly been used to assess these technologies. Advances like human-in-the-loop optimization [24], which adjusts control parameters to optimize outcomes such as metabolic rate, have emerged as promising solutions.

Recently, user preference has been proposed as a "meta-criterion" in device development, allowing stakeholders to guide design based on individual needs, wants, and perceptions. This approach aggregates feedback from users, who offer insights into both functional goals (e.g., speed, exertion) and subjective factors (e.g., comfort, stability), as well as clinicians, who contribute their expertise.

Falling is a serious issue affecting millions, especially those with lower-limb amputations. About one-third of older adults and half of people with limb amputations fall annually [25], often

leading to severe injury or even death, including among younger, active amputees [26]. The fear of falling can also greatly reduce mobility and quality of life.

To mitigate these impacts, fall prevention has become a key research focus. Studies suggest that supporting the hip joint for balance maintenance could effectively reduce falls. Humans use three main strategies to maintain balance while walking: ankle torque to adjust center of pressure, hip torque to control the center of mass, and foot placement to shift the base of support [27]. Since hip torque and foot placement are controlled by the hip joint, a device providing hip torque could enhance balance for individuals with limb amputations, offering broader applicability than ankle-based interventions.

1.2 Significance

The proposed study introduces three innovative contributions aimed at incorporating preference into the control of lower-limb robotic prostheses and providing a novel approach to enhance the gait balance with the mediolaterally active hip exoskeleton for amputee population.

First work introduces a novel framework designed to facilitate user-preferred tuning for a robotic knee prosthesis, addressing the critical need for personalized assistance in prosthesis control. The framework combines a user-controlled interface (UCI) with a reinforcement learning-based algorithm, enabling users to select preferred knee kinematics while the system automatically tunes 12 control parameters to meet those preferences. Through user feedback and blinded comparative studies, the framework demonstrated its ability to meet personalized preferences accurately, with users consistently identifying their preferred knee profile. This approach highlights the importance of integrating user preferences into prosthetic control and shows promise for future applications in both clinical and home settings.

Next, using the framework developed in Aim One, we investigated the top priority for lower-limb amputees, which was found to be gait balance. It led us to aim two. The significance of this work lies in its exploration of how abduction/adduction assistance from a powered hip exoskeleton can effectively modulate step width during walking, a critical factor in maintaining mediolateral balance. By employing a novel admittance control system, the study demonstrates that adjusting the stiffness in the exoskeleton's control can successfully increase or decrease step width without affecting step length. This outcome highlights the potential for wearable robotic systems to enhance balance and stability, particularly for individuals with compromised sensorimotor function, such as lower limb amputees. The findings pave the way for further development of hip exoskeletons that could proactively support gait stability, making it a promising tool for both rehabilitation and balance assistance. We also showed the influence of hip exoskeleton on mediolateral gait balance through modulation of the step width.

Lastly, we developed a novel framework that enables fine-tuning of an offline-trained reinforcement learning (RL) policy with just a single real-time Human-In-The-Loop (HIL) episode. The framework was designed to provide accurate step width control for users of hip exoskeletons, including non-amputees and individuals with lower limb amputation who experience hip muscle weakness. The control system was built to be robust, allowing users to safely override the exoskeleton’s actions, when necessary, while maintaining stability even in the presence of disturbances. Additionally, we demonstrated that this step width control did not increase step width variability, ensuring that the system did not negatively impact balance during walking.

This study is significant for advancing the personalization and effectiveness of lower-limb robotic prostheses and exoskeletons by integrating user preferences and enhancing gait balance. It

introduces innovative control frameworks that enable precise step width modulation and personalized prosthetic tuning, ensuring both improved mobility and stability for individuals with lower limb amputation or hip muscle weakness. The work highlights the potential of incorporating reinforcement learning and real-time user feedback to optimize device performance, making it a promising approach for both rehabilitation and daily use, particularly in addressing balance challenges.

1.3 Outline

The remainder of the dissertation is organized as follows. Chapter 2 introduces a framework for user-preferred tuning of a robotic knee prosthesis, using a user-controlled interface and reinforcement learning to automatically adjust control parameters based on user preferences. This approach successfully meets individual needs, demonstrating the importance of personalization in prosthetic control for clinical and home use. Chapter 3 explores how a powered hip exoskeleton with abduction/adduction assistance can modulate step width to improve mediolateral balance. The study highlights the potential of wearable robotics to enhance stability for individuals with compromised sensorimotor function, paving the way for future developments in gait stability support. Chapter 4 presents a framework for fine-tuning an offline-trained RL policy with a single real-time Human-In-The-Loop (HIL) episode. This system provides accurate step width control while allowing safe user overrides and maintaining stability, without increasing step width variability or negatively impacting balance.

CHAPTER 2

Abbas Alili , Varun Nalam, Minhan Li, Ming Liu , Jing Feng, Jennie Si , and He Huang, "A Novel Framework to Facilitate User Preferred Tuning for a Robotic Knee Prosthesis," in *IEEE Transactions on Neural Systems and Rehabilitation Engineering*, vol. 31, pp. 895-903, 2023, doi: 10.1109/TNSRE.2023.3236217.

2.1 Introduction

Lower limb amputation causes permanent disability, impacting patients physically, psychologically, and socially [28]. Advancing prosthetic technology is needed to enhance individuals' mobility and quality of life with lower limb amputation. One promising technology is robotic prosthetic legs that are motorized and intelligently controlled. Compared to passive alternatives that fail to replicate the behaviors of the healthy limb across various environments, robotic prostheses showed many potential advantages [29], including increased range of motion [30], enhanced stability and balance of wearers [31], [32], and ability to adapt to various terrains [33], [34]. A frequently used control approach for robotic knee devices is a finite-state impedance control (FSM-IC), which can reasonably simulate human limb behavior without complex implementation [35]. Compared to trajectory-based control of robotic prosthesis devices FSM-IC provides more compliance with the user along with flexibility during the operation [36], [37]. However, personalization of the controller's impedance parameters (often over 9) is usually needed and has been one of the main challenges for FSM-controlled prosthesis devices in practice [38]. In the clinic, prosthetists will typically manually tune the parameters to obtain optimal prosthesis control performance in assisting the user's gait [39]. This procedure is highly subjective, time inefficient, and non-standardized. To overcome the limitations of the manual tuning process

of control parameters, an autotuning approach using reinforcement learning (RL) has been proposed by our group for robotic lower limb prostheses previously [6], [40]. The RL-based automatic control method optimally tuned the impedance parameters of each gait phase to replicate the normative profile (NP) of knee kinematics gained from the non-disabled population during gait [41]. Further, this approach has been improved in terms of time efficiency and robustness of the learned tuning policy [42]. The algorithm had been successfully validated with transfemoral (TF) amputees using the robotic knee prosthesis while ensuring their safety. Although promising, one open question is whether reproducing the normative profile of knee motion should be the tuning goal that can satisfy the prosthesis user's preference. Potentially, physiological changes in amputees due to limb amputation and the dynamic difference between the robotic prosthesis and biological limb may lead to different preferred knee kinematics rather than NP [43]. Thus, consideration of the user preference might be important for personalizing the prosthesis control. Studies showed that the lack of user input during the device selection, fitting time frame, and changing user needs are among the main reasons for the prosthesis abandonment [44], [45]. In addition, prosthetists make prosthesis control tuning decisions based on not only the observational gait analysis but also the user's preference and feedback in clinics [46], [47]. These insights signify the importance of prosthesis user's preference consideration in regard to prosthetic behavior. Addressing user preference/satisfaction in wearable robot control optimization has recently become an emerging topic in the research community. Predictive Entropy Search with Preferences algorithm has been developed by Thatte et al. [48] in which user preference is incorporated by pairwise comparisons of different controls. Tucker et al. [49] developed LineCoSpar to learn the utility function via a pairwise comparison of user preferences. The idea was to learn six user-preferred gait parameters of the lower body exoskeleton by considering the user's feedback for

each posterior update. These approaches have finite forced choices from which users select their most preferred behavior. Quesada et al. [50] studied the effect of ankle prosthesis push-off work on the metabolic cost and user satisfaction. Transtibial amputees who participated in the study demonstrated strong preferences over various levels of ankle push-off work despite not experiencing decreased metabolic rates. More recently, approaches where users tune quasi-passive ankle prosthesis stiffness [51] or torque profile of bilateral ankle exoskeleton [52] to find their preferred device control parameters have been successfully demonstrated. These preference-based approaches have been built upon successfully demonstrating perception of users to changes in control parameters of their prosthetic and wearable devices [53]–[55]. These existing studies enabled the researchers to understand the importance of users' preferences in the wearable robot control and also motivated us to include user preference in an FSM-IC control to further leverage the FSM controller benefits. However, one challenge facing us is that the FSM-IC control includes 12 impedance control parameters [10], while all the existing, related studies only explored 1 to a maximum of 6 control/action parameters in the wearable devices. Exploring this high-dimensional device control space by the humans for maximal user preference is difficult, if possible, and has never been demonstrated based on our knowledge. Other solutions that can reduce human adjustable parameter space for FSM-IC controlled device is needed. To address this challenge and enable the tuning of 12 knee prosthesis control parameters to meet the user's preference while ensuring user safety and minimizing human exertion, we proposed a novel hierarchical engineering framework consisting of (1) our previously developed RL-based prosthesis tuning method [16] and (2) a User Controlled Interface (UCI) [56]. The basic working mechanism was that the human users can use the high-level UCI to determine their own preferred prosthesis knee kinematic features in a 4-dimensional space by modifying control points which is then realized by the low-

level RL-based tuning algorithm adjusting all 12 impedance control parameters to meet the desired kinematic features. Since our RL tuning algorithm was time-efficient and the learned prosthesis tuning policy was robust across various kinematic profiles, this framework offered us a unique opportunity to investigate the user's preferences across various knee prosthesis control parameters. Our pilot testing showed the design and feasibility of this engineering framework in adjusting stance phase knee features [56]. In this study, we implemented and evaluated the framework that can tune 12 prosthesis control impedance parameters to meet the user defined features in knee kinematics across gait cycle. Since the perception of users to changes in robot behavior is essential for these users to have a preference, we investigated if users can differentiate between the profile they chose, the normative profile and a random profile to showcase the need for the current framework. Finally, we investigated some potential biomechanical factors that could drive users to choose one profile over the other. The results of this study may lead to a novel wearable robot tuning framework that can personalize high-dimensional device control parameters to meet the user's preference in the future.

2.2 Methods

To achieve the aims of the study, the experiment was designed to evaluate the performance of the framework, by helping users choose a preferred profile and perform comparison studies to analyze users' ability to differentiate different knee profiles. Ten participants, five non-disabled (AB) and five with unilateral above-knee amputation (TF) participated in the study, with demographics as listed in Table I. All amputee participants were community ambulators (K3 activity level or higher) without significant secondary comorbidities, who regularly used conventional passive prostheses and were active in daily life. The study was conducted with the approval of the Institutional Review Board of the University of North Carolina at Chapel Hill, with

all participants providing informed consent. The description of the autotuning framework, experimental protocol, methodologies, and analysis are described below.

TABLE I
DETAILED INFORMATION OF THE SUBJECTS

Subject	Sex	Prosthesis Side	Height (m)	Weight (kg)	Age
AB01	Female	Right	1.86	81.6	23
AB02	Male	Left	1.87	68	21
AB03	Male	Left	1.93	70.3	25
AB04	Male	Left	1.91	75.9	28
AB05	Female	Left	1.90	77.1	20
TF01	Male	Left	1.74	80	23
TF02	Male	Left	1.74	68	42
TF03	Male	Left	1.70	68	67
TF04	Male	Left	1.81	89	38
TF05	Male	Left	1.79	72.5	22

2.2.1 Robotic Knee Prosthesis and User-Controlled Interface (UCI)

A powered robotic knee prosthesis [10] was used for the study. The device relied on a slider-crank mechanism and a DC motor that provided up to 80 Nm of torque at the knee joint and carbon fiber foot with a passive ankle joint. An FSM-IC framework [57] was implemented in the robotic knee to imitate a gait. In this framework, level-ground walking was partitioned into four distinctive gait phases or states: stance flexion (STF), stance extension (STE), swing flexion (SWF), and swing extension (SWE). The control and signal flow architecture of the RL-based UCI is shown in Fig. 1. Trained RL policy adjusts three FSM-IC parameters (stiffness, equilibrium angle, and damping) defined for each gait phase according to the differences between measured features and target features in the knee profile, referred to as the peak error and duration error [42]. The convergence criteria for the autotuning algorithm were to have the four control points (CP1 – CP4) of the knee profile which were appropriate to prementioned gait phases to be within 2 degrees spatially of the target control points and 2% temporally for 6 out of 10 consecutive impedance updates. We integrated the User-Controlled Interface (UCI) into the autotuning architecture (Fig.

1.) that enabled users to interact with the robotic prosthesis by having them set their preferred kinematics for the knee joint. Users were given a remote controller to modify (up and down) the predefined magnitude of four control points corresponding to gait phases shown in Fig. 2(b). The RL algorithm then tuned to this profile while ensuring stability of the user.

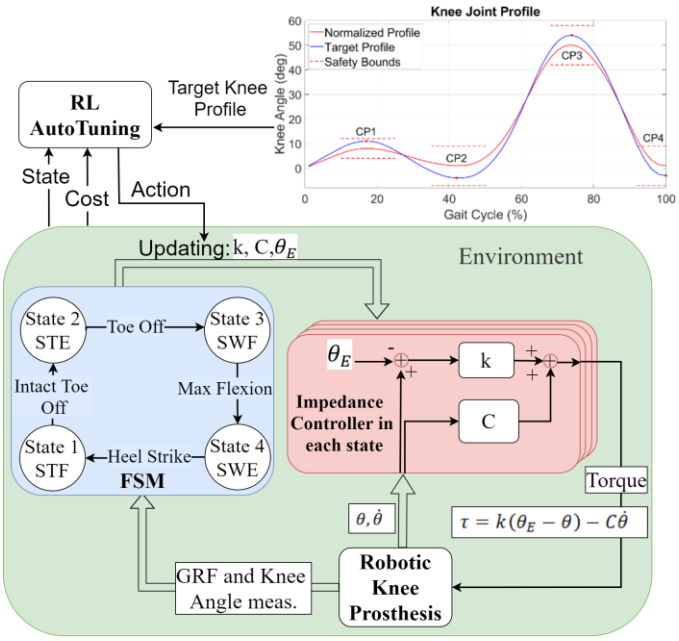

Figure. 2.1. The hierarchical design architecture of the system. Target knee joint profile is sent from a UCI interface to the RL Autotuning algorithm, where the latter updates three FSM-IC parameters for each gait phase accordingly.

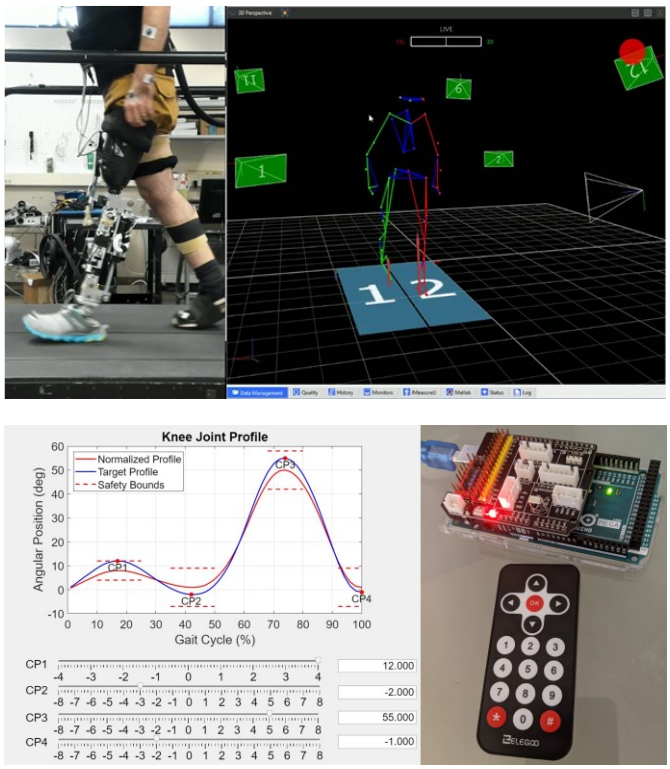

Figure.2.2. a) The experimental setup for the study. The robotic prosthesis worn by the transfemoral subject is aligned and fit by a certified prosthetist. 43 light-retroreflective markers have been used for full-body motion capture. b) User interface and an infrared remote control coupled with Arduino Mega 2560 was used for remote profile modification.

2.2.2 Experimental Setup

The robotic prosthesis used in the experiment was developed for transfemoral amputees Fig. 2(a). To simulate transfemoral amputee behavior in non-disabled populations, an adapter that attaches to the knee while the folded intact limb was used. The powered prosthesis was aligned and fit by a certified prosthetist for amputee users to ensure the comfort and safety of the users. A motion capture system (VICON, Oxford, UK), consisting of 12 cameras sampled at 100 Hz, was used for gait kinematics and kinetics measurement as participants walked on an instrumented treadmill (Bertec Corp. Columbus, OH, USA). According to the Newington-Helen Hayes full-

body gait model [58], we utilized 43 light-retroreflective markers placed on the participant's head, trunk, pelvis, and bilaterally on the thighs, shanks, and feet. Bilateral ground reaction forces (GRFs) were recorded at a sampling rate of 1000Hz by an instrumented split-belt treadmill synchronized with the motion capture system for biomechanical and inverse dynamic analysis to evaluate gait behavior.

2.2.3 Experimental Protocol

The experiment duration was two consecutive days for each participant and was divided into the following sessions: profile exploration and pairwise blinded profile comparison sessions. In the first session, the users were fitted with the prosthesis, which was then tuned to simulate a normative knee kinematic profile (NP). Then to familiarize the participants with how changing the control point location affects the robot behavior, we let the participants explore different profiles in which one of the four control point was changed while the rest were set to NP. They were first instructed to move the first control point above its NP location by 3 degrees and the resulting profile was tuned. Then they are instructed to move the control point below its NP location by 3 degrees and the tuning is performed. The process is then repeated for the remaining three control points resulting in tuning of 8 profiles, two for each control point. It should be noted that each control point has been tuned in isolation from the other three. To reduce fatigue, a 2-minute rest was provided for each participant after every 2-minute interval of walking on the treadmill for tuning trials. Upon completion of the tuning of the nine profiles (one NP and eight modified profiles), subjects were then instructed to experience each of the profiles so that they understand how moving the control point affects robot behavior. This was achieved by instructing the participants to walk on the treadmill with the powered prosthesis replicating NP, +3 ◦ and -3◦ profile for each control point for 45 seconds. As a result, each participant walked in twelve 45

seconds of treadmill walking bouts where NP profile repeated four times. At the end, the subjects were also asked which of the three profiles they prefer for each control point, and their preference was noted. Thus, at the end of these search trials, we were able to construct a starting point for preferred knee joint profile according to participants' preferences regarding each phase. For the second session, the robotic prosthesis was fit to the user and was tuned again to replicate NP to account for differences in socket fitting. Then the prosthesis was tuned to the constructed profile acquired using the preferred control points' locations from the previous day. This profile is constructed by joining the selected control points using minimum jerk profiles. Once tuned, the participant walked with this profile to verify if they were satisfied with it or if any adjustment was needed. Any adjustments were then incorporated, and the resulting profile was tuned. Once the participant was satisfied with the profile, the control parameters were saved as the person's preferred profile (PREF). Finally, in order to eliminate the random choice effects during the blinded comparison session (detailed below), we tuned a profile called opposite profile (OPP). OPP profile mirrored the preferred profile with respect to the NP, e.g., if a participant chose +3 ◦ for a CP1, then the OPP profile is tuned to -3◦ at that control point and vice versa. Once the three profiles were tuned, 12 pairwise blinded comparisons (4 sets of each of the three pairs: NP vs. PREF, NP vs. OPP, PREF vs. OPP) were held at the end of the second session. The goal was to investigate if subjects can actually perceive the differences between profiles and have a preference when they are blinded to the profile they are experiencing. To minimize the order effect, the order of the pairwise comparisons and the order of the trials in the pairwise comparisons were randomized for each participant. Each participant was asked to walk with both profiles in a pair for 45 seconds without knowing which two profiles out of three they were experiencing. After experiencing 45 seconds of walking for each profile, participants were asked about which of the

two profiles they preferred for walking and if they could recognize them. The consistency of preference and user's ability to recognize profiles was then analyzed. They were allowed to skip the recognition of any profile if it was truly hard for them to recognize (NP, PREF, or OPP)

2.2.4 Data Analysis and Evaluation Metrics

The proposed autotuning framework was evaluated by quantitative and qualitative aspects. First, we quantified the performance of the RL-learned tuning policy by (1) the success rate in meeting targeted knee kinematics (i.e., effectiveness) and (2) the duration needed to meet targets (i.e., time efficiency) after the targeted knee profile was modified. In addition, we quantified UCI usability by a qualitative survey with items adapted from the System Usability Scale [59], consisting of 9 questions and the space for general feedback. To quantify the consistency of participants' perceptions about their chosen profile, the percentage of chosen profiles during the blinded pairwise comparison was calculated. The aim was to provide insights about the choices of profiles over each other (NP vs. PREF, NP vs. OPP, PREF vs. OPP). In addition, we quantified the number of times when participants were able to recognize or mislabel the experienced profiles. In addition to exploring the user's perception on various profiles, some possible biomechanical factors that could influence the subjects' preference for a profile were analyzed. To that effect, temporal and step length symmetry [60], and margin of stability [61] were analyzed. Joint kinematics and kinetics were calculated using the conventional inverse dynamics approach with the Plugin-Gait software (PiG, Vicon, Oxford, UK) [15], [62]–[64]. MATLAB 2020a was used to obtain a symmetry and stability index for further data analysis. Thirty-five seconds of steady-state gait data from the pairwise comparisons were analyzed for each profile to analyze these factors. A fourth-order Butterworth filter smoothed GRF signals with a cutoff frequency of 25 Hz to reduce noise while the marker positions were low-pass filtered by a fourth-order Butterworth filter with a

cutoff frequency of 10 Hz. The data was then split into gait cycles using the GRF of each limb with a threshold of 30 N. The average gait cycle data was then evaluated using (1) to evaluate temporal and step length symmetry.

$$SI = \frac{x_i - x_p}{(x_i + x_p) * 0.5} * 100\% \quad (2.1)$$

where SI – symmetry index, xi and x p are intact and prosthesis side parameter (i.e., step length or stance time in this study). The value of SI = 0 indicates perfect symmetry. Dynamic margins of stability measures were adapted from Hof et al. [65] based on the extrapolated center of mass (XcoM) equation shown below:

$$XcoM = y + \frac{\dot{y}}{\omega_0} \quad (2.2)$$

$$\omega_0 = \sqrt{\frac{g}{l}} \quad (2.3)$$

where y is the COM position in sagittal plane, $\dot{y}$ is the COM velocity and ω0 is the angular frequency of the approximated inverted pendulum estimated through (3), in which g is the acceleration due to gravity, and l is the equivalent pendulum length, which was taken 1.34 times the leg length in this study [66]. The dynamic margin of stability (MOS) was then defined as:

$$MOS = XcoM - BOS \quad (2.4)$$

where BOS was the boundary of the base of support (i.e., the most anterior edge of the leading foot). We further defined the anterior-posterior (AP) margin of stability (MOS AP) as the AP distance between the XcoM and the toe marker of the leading foot. To determine significant differences among compared biomechanics metrics, interparticipant mean and standard error for each compared knee joint profile were calculated across all participants and the Friedman test was performed accordingly.

2.3 Results

2.3.1 Autotuning System Performance

Based on the criteria set for control tuning convergence mentioned in the methods, the RL-learned tuning policy could achieve 100% successful rate to tune the prosthesis knee control parameters to meet various target profiles chosen by different subjects, showcasing the robustness of the algorithm. The time duration required to tune all tested prosthesis profiles among all participants was 2.5±1.4 minutes. That means after each prosthesis targeted profile change (via UCI), it took around 2-3 minutes of walking for RL to tune prosthesis control to reach the new targeted knee motion. Fig. 3. (a) shows the representative convergent behavior of the RL auto-

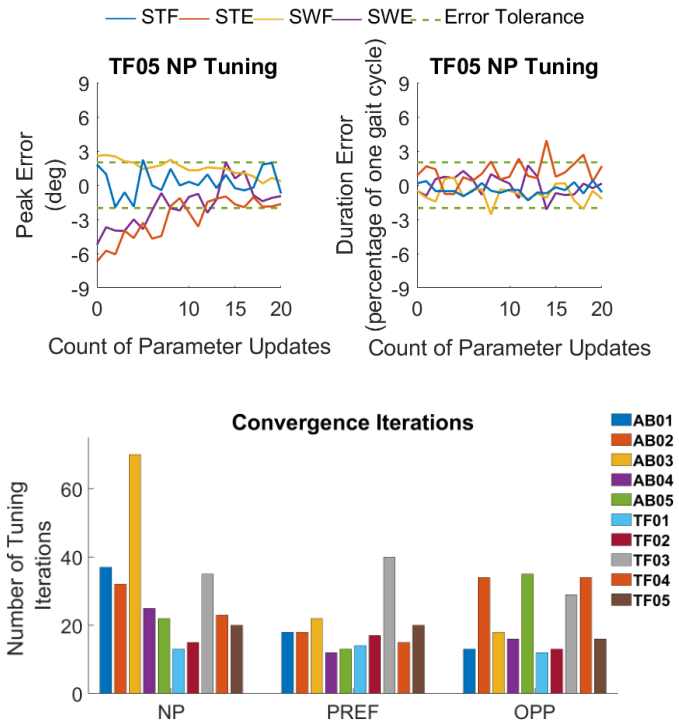

Figure. 2.3. a) Representative figure showing the spatial and temporal convergence of the RL algorithm to tune the 12 control parameters of robotic prosthesis according to NP kinematics provided. b) Number of tuning iterations needed to achieve the full convergence over three profiles and all participants. One tuning iteration constitutes to four gait cycles.

tuning algorithm for NP profile tuned for TF05 whereas Fig. 3. (b) demonstrates the number of iterations needed to tune all three profiles for all participants. It should be noted that each iteration constitutes to four full gait cycles. Table II summarizes the response of the participants to questions

TABLE II
UCI USABILITY SURVEY RESULTS

1.	I found the UCI unnecessarily complex.	**7**	**3**	**-**	**-**	**-**
2.	I thought the UCI was easy to use.	**-**	**-**	**2**	**2**	**6**
3.	I think that I would need assistance tobe able to use the UCI.	**3**	**3**	**2**	**1**	**1**
4.	I found the various functions in the UCI were well integrated.	**-**	**1**	**1**	**7**	**1**
5.	I thought there was too much inconsistency in the interface.	**5**	**4**	**1**	**-**	**-**
6.	I would imagine that most people would learn to use this interface very quickly.	**-**	**2**	**-**	**5**	**3**
7.	I found this interface very cumbersome/awkward to use.	**4**	**4**	**1**	**1**	**-**
8.	I felt very confident using this interface.	**-**	**-**	**1**	**6**	**3**
9.	I needed to learn a lot of things before I could get going with this interface.	**6**	**2**	**2**	**-**	**-**

asked for the evaluation of the UCI usability. The number in each box denotes the number of participants who gave the rating to the specific question. 7 out of 10 participants agree that the UCI was easy to use and could be learned to use very quickly.

2.3.2 User Preferred Knee Profiles

Fig. 4. shows the preferred profiles for each of the participants along with the normative profile as a comparison. Eight out of ten participants preferred the CP1 to be different from that of NP, with 7 of them choosing a lower knee angle value. In comparison, 9 out of 10 participants chose a different location for CP2, while only 5 and 7 subjects chose a different profile for CP3 and CP4 respectively. Looking into the preference, six participants (4 TFs) preferred to increase the second control point (CP2) whereas three of them (1 TF) decided to decrease it. For the last

control point, there were no particular trend. On an individual basis, four participants (AB02, AB03, TF03 and TF05) preferred to achieve a relatively flat trajectory for the stance phase with similar values for CP1 and CP2. Additionally, four participants (AB03, AB05, TF02 and TF04) preferred to increase the CP4 while decreasing the CP1. Overall, there was no particular profile preference trend observed among all the participants.

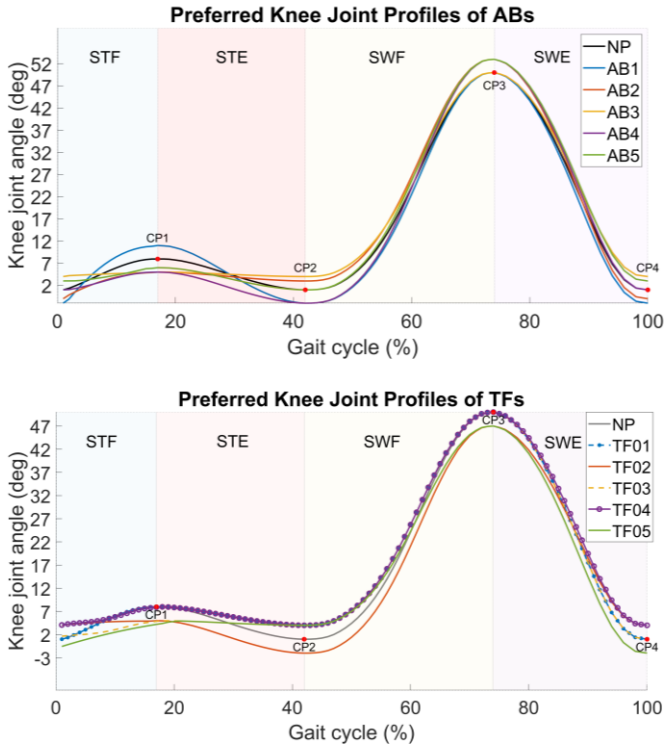

Figure 2.4. Preferred knee joint profiles for non-disabled (AB) and amputee (TF) participants are shown along with normal knee joint profile. Control points are shown with red dots. Plots are divided into four gait phases: stance flexion (STF), stance extension (STE), swing flexion (SWF), and swing extension (SWE).

2.3.3 Pairwise Comparison Analysis

In accordance with the study's aims, once the preferred profile was obtained, the participants' ability to consistently perceive different profiles and recognize their preferred profile

was evaluated. The distribution of participants' choices upon pairwise comparison of their preferred profile, NP and OPP profiles is shown in Fig. 5. Participants chose the preferred profile over the opposite profile almost in all comparison trials. Participants also chose the preferred profile over NP 89% of the time. The choice rate of NP over OPP profile was 66%. The comparison results suggests that users can physiologically differentiate between the profiles and have distinct preferences. A confusion matrix based on profile recognition data combining all the subject responses was developed and shown in Table III. It should be noted that the cases that participants could not recognize the experienced profile are excluded from the calculation of the confusion matrix. Since each subject experienced each individual profile (NP, PREF and OPP) 8 times during the comparison tests, there were a total of 80 datapoints. Participants were able to recognize the preferred profile with a 73.8% recognition rate. Around 18.8% of the tested preferred profile was

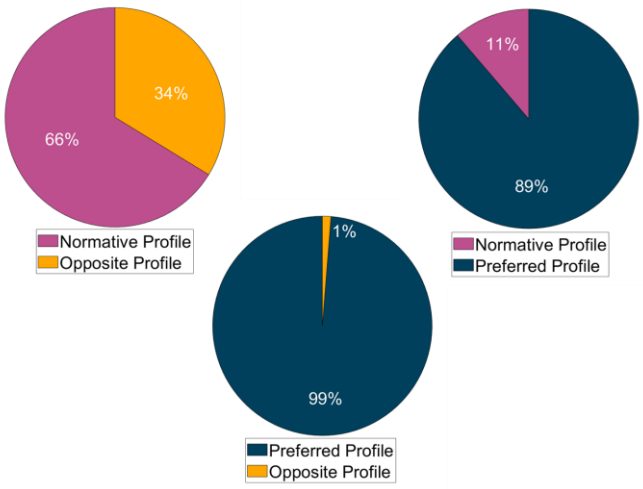

Figure 2.5. Pairwise profile choice results show the percentage of each chosen profile for all 10 participants. NP has shown with pink, PREF with blue and OPP with yellow color.

mislabeled as NP, and only 3.8% of the tested preferred profile was recognized as the opposite profile. The opposite profile was correctly recognized in about 63.8% of cases. Most of the confusion errors occurred between the opposite profile and NP. The comparison between Fig. 5.

and Table III shows that even in cases where the profile wasn't recognized, there was a preference for PREF profile over other profiles.

2.3.4 Biomechanical Analysis

Lastly, we explored gait symmetry and balance index that may potentially be correlated with the users' preferences in prosthesis control. Only TF data is reported here. The interparticipant

TABLE III
PROFILE RECOGNITION CONFUSION MATRIX

		True Profiles		
		NP	PREF	OPP
Recognized Profiles	NP	38.8%	18.8%	28.8%
	PREF	16.3%	73.8%	5%
	OPP	41.3%	3.8%	63.8%

mean and the standard error (SE) across participants for the stance time and step length symmetry indexes across three knee joint profiles is shown in Fig. 6. along with similar measurements for

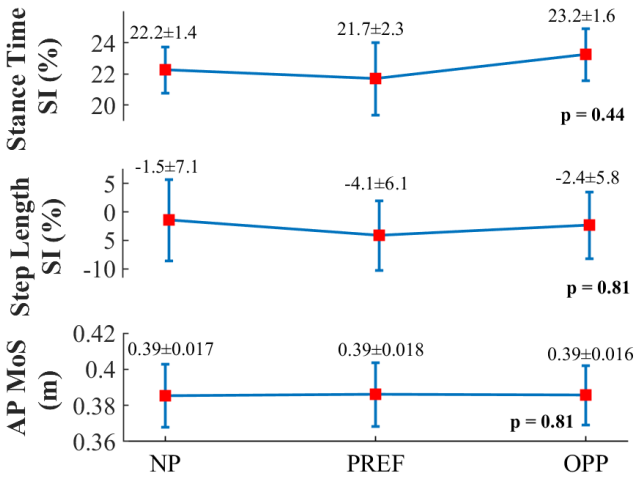

Figure 2.6. Red squares and blue error bars represent the TF interparticipant mean and standard error (over eight trials) for each knee joint profile for (a) stance time (b), step length symmetry indexes, and (c) margin of stability in the anterior-posterior direction. The p-value for each compared metric is shown at the top of each graph.

the margin of stability in anterior-posterior direction. The Friedman test across 5 TF participants over 8 trials for each knee joint kinematics showed no significant differences for all three indexes utilized (Fig. 6.).

2.4 Discussion

In this study, we demonstrated the function of UCI, hierarchically combined with the RL-based prosthesis tuning algorithm, to tune 12 prosthesis control parameters that can be potentially used to tune the kinematic behavior of the robot based on user's preference. In addition, the study showed that users can perceive different profile and given a choice, their chosen profile is generally different from a normative profile, implying the need to consider user preference. Further, understanding the user's decision-making process in selecting preferred knee kinematics features and the gait biomechanics associated with the user's preference could provide additional insights to the future development of controller and tuning algorithms that align with user preferences, thereby leading to better technology adoption. Finally, some preliminary biomechanical analysis has been performed to investigate if there is a specific factor that leads to users preferring one profile over the other.

2.4.1 RL Based Autotuning Algorithm and UCI Framework

According to the results of the study, the RL-based autotuning algorithm demonstrated its time efficiency and robustness of the learned prosthesis tuning policy across various kinematic profiles. Without re-updating the tuning policy, when the knee kinematics profile changed, the algorithm could tune the 12 control parameters in under 40 iterations for most subjects safely to reach the new target profile. The ability of the algorithm to tune over the high-dimensional device control space suggests the possible feasibility of the approach being deployed outside of the laboratory settings to tune prosthesis control parameters according to target knee joint kinematics.

In addition, participants' responses to the UCI usability survey showed that the interface was easy to use, and the users were confident when using the interface. However, the participants required additional explanation of the meaning of the knee kinematics associated with their walking. This could be addressed by developing a detailed video to explain gait and knee features in layman's terms prior to their UCI based tuning session.

2.4.2 Preferred Profile Analysis and User Preference

Results showed that the preferred knee motion curves were unique for each participant. While replicating NP using a robotic prosthesis has been the current predominant approach, none of the participants preferred the NP. Based on the profiles, while some participants preferred a more rigid prosthetic during the stance phase, others preferred a more compliant approach by having higher flexion of the knee before the heel strike that was immediately changed to a more rigid extension. However, no explicit assertions were observed in user feedback, although some users mentioned stability and lack of wobble as their driving factors, which could explain the preference of stiffer prosthesis. This observation implied that users had a specific preference even if they might not verbalize the specific qualities that they were looking for. It also highlighted the importance of having an approach that can let the prosthesis users explore different possibilities of prosthetic behavior. In addition, the profile exploration trials for this study have been performed sequentially and there was no way for participants to assess how changing one control point changes their perception of the others. Thus, our ongoing study aims to analyze the psychological aspects that can drive prosthesis users' choices during the extensive exploration of their preferences while also considering the interdependent relationships between control points that could affect profile perception [67], [68]. In most cases, participants successfully chose their preferred knee profiles during the blind pairwise comparison session, supporting the assumption

that participants were able to physiologically differentiate between the experienced profiles. In addition, participants were able to recognize their preferred knee profile with moderate accuracy, even with limited exposure. This observation implies that clinicians and robotic prosthesis manufacturers could rely on the consistency of users' opinions for tuning the prosthetic. Given the effectiveness and time efficiency of our proposed framework to tune prosthesis control based on user's preference and the consistency in the user's perceived preferences, our framework may be potentially used by the prosthetists in clinics and even be transferred to home for prosthesis users. In addition, all the sensing in the tuning algorithm being internal to the device makes it a possible solution for clinics and home environment because extensive gait analysis instrumentation tools are not easily available in such healthcare facilities. However, practical challenges related to the hardware and safety need to be addressed before the system can be implemented at home. One of our future works is to let prosthetists use the software and provide feedback on our design.

2.4.3 Biomechanical Analysis

Effects of user preferred prosthesis control on gait performance metrics related to gait symmetry and stability were preliminarily examined. The main gait performance metrics chosen for analysis were symmetry (stance time and step length) and balance (margin of stability). These factors were chosen based on their impact on the amputee users. It has shown that gait asymmetry causes long-term health conditions [69]. Further, the loss of somatosensory feedback and proprioception results in reduced balance confidence [70]. Unfortunately, no clear and consistent effect was observed across participants. The user preference was not clearly reflected in terms of gait biomechanics metrics, explored in this study. Although the user verbally expressed that gait stability was the factor in their reported reference, we did not observe consistent, large change of AP gait Margin of Stability for preferred control, compared to the other two control settings. This

was potentially because the human's perceived walking instability is more sensitive than the measured balance metrics, as also observed in our previous study [71]. Another limitation was we only explored one stability index. Potential biomechanical variables that are more sensitive to balance instability than MOS should be considered, which could be a potential future work.

2.5 Conclusion

The study showed the feasibility of a novel hierarchical autotuning framework that can effectively and efficiently tune 12 robotic knee prosthesis control parameters to meet the user's preference while ensuring their safety. In addition, with the advantage of the utilized framework for selecting preferred prosthesis control, we showed that prosthetic knee users could consistently distinguish between different profiles tuned using the interface and displayed consistency in preference between these profiles. These results, although from a limited number of study participants, suggested that our framework has the potential to enable prosthesis users or clinicians to integrate the user's own perceptions and preferences into a prosthesis tuning procedure, simplified by the RL-based tuning algorithm. It should be noted that the preference studies include able bodied individuals, since the focus was on investigating if they can physiologically differentiate the different profiles. So, we cannot make any behavioral assertions on specific choices for the profiles. Furthermore, the preliminary gait biomechanical analysis showed that user preference was not clearly reflected in terms of the gait biomechanics metrics that we explored in this study. Due to the limited sample size (5 TF participants) and biomechanical metrics explored, additional biomechanical research is needed to understand the association of user preference with the gait performance measures. Beyond the limitations discussed in the Discussion section, we also identified several other limitations and future work. Our experiments were conducted in a short timeframe. Further research is needed to answer the question about the consistency of

preference over a longer timeframe. In addition, the explored gait performance measures were all only related to gait kinematics in this work. Computing the joint kinematics or monitoring EMG signals in the biomechanical analysis is needed in the future. Our study allowed changes only at control points that are fixed in gait phase for the participants to tune their prosthesis knee profile. In the future, we aim to provide participants a continuous knee feature space to explore when tuning the self-selected prosthesis control. Finally, one unexplored path that has the potential to further reduce the tuning time would be to investigate the sensitivity of users to different control points. Identifying the sensitivity to changes in each control point and how changes in one control point affect perception of other control points could inform the design of future preference-based tuning such as the angular resolution and the number of control points. The successful investigation of such kind of sensitivity could further accelerate exploration and ensure people with amputation can personalize their prosthetic behavior with ease and efficiency.

CHAPTER 3

A. Alili, A. Fleming, V. Nalam, M. Liu, J. Dean and H. Huang, "Abduction/Adduction Assistance From Powered Hip Exoskeleton Enables Modulation of User Step Width During Walking," in IEEE Transactions on Biomedical Engineering, vol. 71, no. 1, pp. 334-342, Jan. 2024, doi: 10.1109/TBME.2023.3301444.

3.1 Introduction

Human walking is one of the most critical activities toward independence in daily life. However, bipedal walking is an inherently unstable activity [72]. To overcome that instability humans need to continuously control their balance in mediolateral (ML) and anteroposterior (AP) directions to achieve smooth and stable walking [73]. It has been demonstrated that individuals can maintain balance during walking against perturbations in the AP direction largely via passive dynamics of the human body, while active motor control is required for managing the perturbations occurring in the ML direction [74], [75]. When sensorimotor integration or muscle strength is disrupted, as observed in older adults, post-stroke patients, or people with multiple sclerosis, the ability to maintain mediolateral stability is usually negatively impacted [76], [77]. Loss of balance in the ML direction can lead to falls and serious injuries [78], [79]. Therefore, interventions or technologies that can address balance control in ML direction in walking are needed. People maintain balance in the ML direction during gait via several strategies [80], including active control of step width [81]. Rankin et al. [82] previously demonstrated that step width behavior during walking is likely the result of sensorimotor integration of stance leg position relative to the position of the center of mass on a step-by-step basis. It has also been shown that individuals primarily use the hip joint to modulate step width during gait, where the gluteus medius (GM)

muscle activation is the most correlated to step-by-step behavior [83], [84]. In that way, hip joints can also influence the center of mass position and velocity to achieve a stable gait [85]. Humans also modify their step width behavior under various contexts that challenge balance to reduce the risk of falls. For example, individuals increase their step width when larger gait perturbations are expected to happen [86]. Increasing step width also alleviates the consequence of imprecise previous foot placement (i.e., step width) during gait [75]. Impairment to any of these components of step width modulation (e.g., GM weakness, impaired sensorimotor integration) hinders step width modulation as a feasible resource for individuals to maintain ML balance during walking [87]. Poor gait stability in several populations has been linked to changes in step width behavior. Older adults tend to walk with wider and more variable steps [85]. Similarly, individuals with lower limb amputation or post-stroke patients exhibit a gait with larger step width compared to non-disabled peers [88]–[91]. It has been postulated that this behavior is a result of poorer sensorimotor integration, where individuals after stroke fail to accurately integrate the position of their stance limb and pelvis to then place their swing foot appropriately [92]. Despite increased metabolic cost [93], [94], these populations prefer to walk with wider steps, implying the prioritization of stability and balance during the gait. This relationship between step width behavior and gait stability among several populations makes modulation of step width a potential target for assistive or rehabilitative systems to improve balance. Various engineering systems have been developed to control the step width for clinical populations for study of balance control mechanisms or rehabilitation purposes. External, lateral stabilization tools have been developed by different groups to investigate step width and its variability [85], [95]. Pennycott et al. [96] decreased individuals' step width by a robot-driven gait orthosis aimed to be used for balance rehabilitation of neurologically impaired people. Heitkamp et al. [97] directly modulated foot

placement of post-stroke patients during gait through a cable-actuated force-field to investigate the potential assistive and rehabilitative effects. They demonstrated success in improving step-by-step foot placement using an assistive force-field for guided foot placement in post-stroke patients. Additionally, by using a resistive force field (i.e., moving patients' foot placement away from the appropriate location) participants improved step width behavior once the force-field was removed. These efforts have demonstrated the potential to successfully modulate step width behavior; however, these immobile test beds are limited in their potential for use outside of the laboratory. Another emerging technology to assist walking balance is wearable robotic powered exoskeletons [98]. Since hip joints are important for gait stability [80], [84], several hip exoskeleton systems have recently been developed and tested. Monaco et al. [99] designed a novel control algorithm governing active flexion/extension hip exoskeleton to prevent elderly people and transfemoral amputees from falling after perturbations. A unified active control framework of 2-DOF hip exoskeleton acting in AP direction has been proposed by Qiu et al. [100] for both walking and balance assistance. They were able to show that the proposed system was able to mitigate push and pull perturbations. Contrary to hip exoskeletons acting in the AP direction, there are a very limited number of hip exoskeletons available that demonstrated balance assistance in the ML direction during the gait. Zhang et al. [101], [102] showed the feasibility of the proposed 4-DOF hip exoskeleton that reacts to standing balance perturbations and produces a compliant guidance force. Chiu et al. [103] developed a bilateral hip exoskeleton emulator to further investigate potential ways to assist users' behavior during walking or perturbation recovery. Although exciting, the goal of these studies was to use hip exoskeleton control to reactively assist to the recovery of walking stability after perturbations in gait. There have been limited number of studies to explore the potential of wearable robots to proactively assist the modulation of step width in

natural strides for improved ML balance in regular walking. Thus, many research questions exist before enabling proactive step width manipulation via a hip exoskeleton, e.g., what should be the exoskeleton control and configuration? How do human wearers respond to the exoskeleton's action? The objective of this study is to address these knowledge gaps before developing closed-loop control of wearable robots to enable step width regulation. In this study, we presented an active hip exoskeleton that powers hip abduction/adduction bilaterally via admittance control. By adjusting admittance control parameters during natural walking, we investigated the human step width response to our active hip exoskeleton. We showed success of our powered ML hip exoskeleton and control in increasing and decreasing the step width during walking without causing a change of step length in healthy individuals. In addition, we examined the activity of hip abductors (i.e., the gluteus medius) to understand the human's hip ML control efforts in changing of step width in the experiments. The results of this study implied the promise of using an active abduction/adduction hip exoskeleton and admittance control parameter change to modulate step width in natural strides. The outcome also informs the high-level control design of hip exoskeleton that can regulate the step width for proactive gait balance interventions in the future for individuals with balance deficits.

3.2 Methods

3.2.1 Participants

Ten non-disabled, neurologically intact adults (6 males, 4 females; age = 25.2 ± 4.6 years; mass = 70.8 ± 11.6 kg; height = 1.72 ± 0.06 m; mean ± s.d.) participated in this study. The study was conducted with the approval of the Institutional Review Board of the University of North Carolina at Chapel Hill (133028), with all participants providing informed consent.

3.2.2 Equipment: ML Hip Exoskeleton

A fully powered and compliant 2-DOF robotic ML hip exoskeleton developed by Neuromuscular Rehabilitation Engineering Laboratory (NREL) was used in this study [104]. During the design process, we utilized a modular motor design and employed a low-level admittance control mechanism. The device was equipped with two brushless EC flat motors (Maxon, USA) acting on a hip in the frontal plane (Fig. 1(a)). Passive hinges enabled free movement of the legs in the sagittal plane. The exoskeleton system uses a harmonic gearbox (CSD-20-100-2A-GR-SP674, Harmonic Drive, MA, USA) providing a 100:1 transmission ratio. The hip exoskeleton can produce an output torque of 34 N·m, and a peak torque of 57 N·m. The hip abduction/adduction angle was measured by the encoder (Maxon, USA) attached to the motor. The interaction arm connecting the actuator to the limb. The hip exoskeleton was worn around the waist and fastened to the thighs of the participants through cloth cuffs as shown in Fig. 3.1(a).

3.2.3 Admittance Controller for Hip Exoskeleton Actuators

To ensure safe physical human-exoskeleton interaction, we used admittance control [105] for each actuator to power hip abduction/adduction, as shown in Fig. 3.1(b). Admittance controllers used virtual impedance parameters, such stiffness (K), damping (B), equilibrium angle (θeq), and inertia (M) to model the dynamics of human-exoskeleton system. Admittance control, according to the observed interaction torque (τ_{int}), determines the angular velocity reference signal for the low-level controller to produce required motor torque. (1) describes the dynamics for interaction torque τ_{int}(t), where θ represents the measured exoskeleton hip abduction/adduction angle, and ˙ θ(t) and ¨θ(t) are its derivatives standing for motor velocity and acceleration respectively:

$$\tau_{int}(t) = M\ddot{\theta}(t) + B\dot{\theta}(t) + K[\theta(t) - \theta_{eq}] \tag{3.1}$$

The control was implemented on a real-time PC using EtherCat (TwinCAT 3.1) protocol executing at 1000 Hz.

In this study, we used two parameters of the admittance controllers (K and θ_{eq}) to study the human step width response to different exoskeleton mechanics. M and B were fixed at 0.2 and 0.3 values respectively. The equilibrium angle was utilized to define the direction of the applied torques in terms of abduction or adduction of the hip joint as shown in Fig. 1b. We aimed to explore a large range of step-width behavior, both in the abduction and adduction directions, thus we selected an equilibrium angle beyond the widest ($\theta_{eq,Ab}$) and narrowest ($\theta_{eq,Ad}$) ML hip joint excursions that shown in literature [106]. Therefore, we opted to use double the reference value (~7°) to ensure that the necessary torque would be applied for both increasing and decreasing the step width of hip exoskeleton users. Once these angles were established, they were set to a constant value (15°) for the whole gait cycle to systematically investigate various stiffness values.

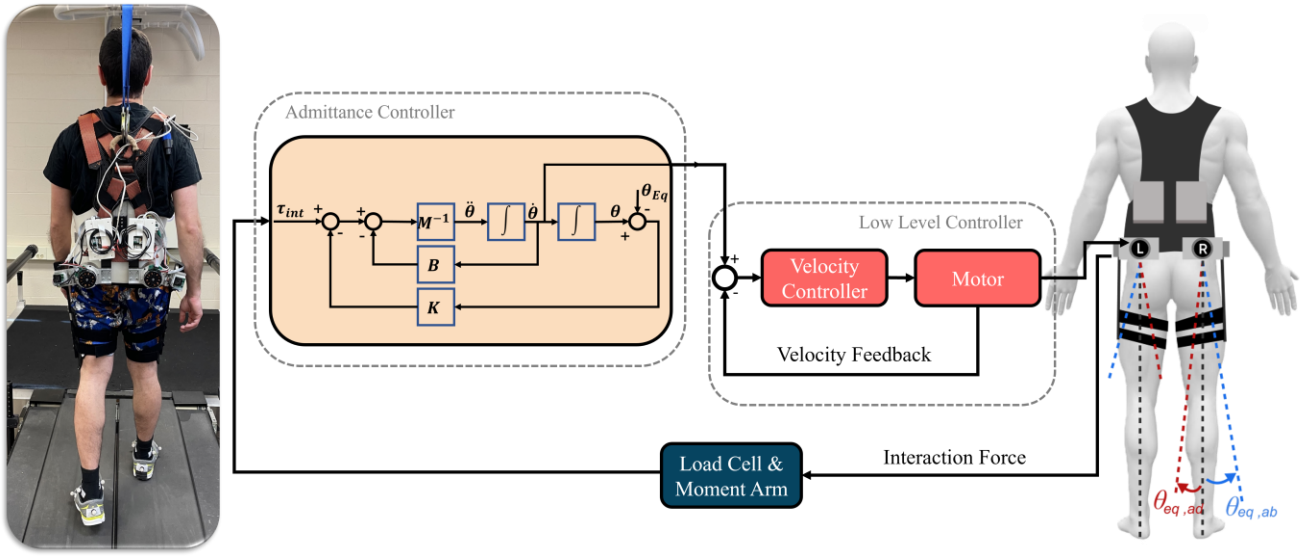

(a) (b)

Figure 3.1. (a) The ML Hip Exoskeleton applied abduction/adduction torque during the whole gait cycle. Participants were instructed to walk comfortably. (b) Admittance control diagram used to assure safe human-device interaction. The equilibrium angle parameter is used to define the direction of the applied torque according to modulated stiffness values.

Essentially, we modified different stiffness coefficient (K) for either direction to produce different interaction behavior.

When K is equal to zero, i.e., zero impedance (ZI) mode, the ML hip exoskeleton aims to match the hip joint movement of the human wearer without any extra torque applied. When stiffness K increases, the abduction/adduction torque applied in the direction of the predefined equilibrium angle increases.

3.2.4 Experimental Setup

A motion capture system (VICON, Oxford, U.K.), consisting of 12 cameras sampled at 100 Hz, was used to track foot positions while participants walked on an instrumented treadmill (Bertec Corp. Columbus, OH, USA). As shown in Fig. 1(a), participants wore a safety harness attached to an overhead rail, which did not provide body weight support. Twelve light-retroreflective markers were placed on the participant's feet (the second toe calcaneus, first and fifth metatarsals, lateral and medial malleolus, and heel of each foot). Ground reaction forces (GRFs) were recorded at a sampling rate of 1000Hz by an instrumented split-belt treadmill synchronized with the motion capture system to detect the gait events. Detected gait events were visually inspected during the processing of the data to avoid missing heel strikes and toe offs. It has been demonstrated that the gluteus medius (GM) muscles play a crucial role in modulating step width [107], [108] when humans voluntarily adjust their step width. Additionally, these muscle groups exhibit the highest level of activity during ML foot placement [84]. These findings served as the foundation for our investigation into the behavior of GM muscles. Thus, electromyographic (EMG) signals of the GM muscles during the treadmill walking was measured bilaterally by bipolar surface electrodes (Motion Lab Systems, Louisiana, USA) sampled at

1000Hz. SENIAM [109] guidelines were used for the placement of the electrodes after cleaning the skin surface with alcohol.

3.2.5 Experimental Protocol

We investigated the effects of the active torque application of the hip exoskeleton in the abduction/adduction direction for the entire gait cycle on human's step width. The decision to apply abduction/adduction torque throughout the entire gait cycle was based on research findings that demonstrated the role of the GM in controlling step width both in stance and swing phases. The experiment was carried out in one day and divided into three sessions: acclimation, abduction assistance, and adduction assistance. To ensure efficient human-device interaction, first, all participants were asked to walk on the treadmill while the hip exoskeleton was in a zero impedance (ZI) mode at their self-selected walking speed. The self-selected walking speed was determined by gradually increasing the treadmill speed in increments of 0.1 m/s until the participant verbally confirms that it was their preferred speed. The participant's self-selected treadmill speed was set constant throughout all sessions to avoid any impact of walking speed on step width [110]. We allowed participants to acclimate walking with the hip exoskeleton in the ZI mode for 2 walking trials (3 minutes each). Then participants were asked to walk for three trials, wearing the device, for both abduction and adduction assistance conditions. Each abduction or adduction walking trial was 5.5 minutes long with the ZI mode control for the first thirty seconds. In each trial, participants experienced 5 levels of stiffness K: 0, 20, 40, 60, and 80 N·m/rad. We applied each stiffness level for 1 minute of the walking trial for both left and right joints and randomized the order of K levels for each individual trial. Ultimately, each participant experienced the same level of K three times for each of the abduction or adduction assistance sessions. These levels of K were chosen empirically based on pilot study work.

3.2.6 Data Processing, Evaluation Metrics, and Statistics

The marker positions were low-pass filtered by a fourth-order Butterworth filter with a cutoff frequency of 10 Hz. GRF signals were low-pass filtered with a cutoff frequency of 25 Hz. Heel strike events were identified using the GRF of each limb with a threshold of 30 N [111]. We computed step width and step length based on maker positions. The step width was calculated as a mediolateral distance between heel markers at each heel strike [107]. Similarly, step length was defined as an anteroposterior distance between heel markers at each heel strike. Only the last 40 seconds of the step width data relevant to each K level was analyzed for the steady-state behavior to avoid the transient effects.

The calculation of linear correlation coefficient (Pearson's r) is conducted using JMP, Version 17.0.0 (SAS Institute Inc., USA). The data used for the analysis consists of the averaged steady state step width values for all participants across the modulated stiffness values. We were also interested in investigating how quickly humans react to the K change when this change led to significant step width modification. First, we selected the K changes that led to significant step width adjustment. To quantify how quick is the human reaction, we defined the reactive strike number right after a K change using Cusum Control Chart (CuSum) method [112], [113]. Using cusum function in MATLAB (MathWorks, USA) allowed us to identify the first strike that shows the significant shift of mean from the step width derived from the strikes before K change. The number of these identified strikes after the K change was defined as the reactive strike number. The details about cusum algorithm and its implementation is shown in Appendix. To evaluate muscle activity, we computed the EMG envelope of bilateral GM. EMG envelope was obtained by filtering raw EMG signals with a high-pass filter (cutoff at 20Hz, 4th order), followed by rectification and low-pass filtering (cutoff at 50Hz, 4th order). We then segmented EMG for both

the left and right GM based on the timing of left and right heel strikes. We normalized EMG envelope in time for each gait cycle (heel strike to heel strike of the same limb). To compare EMG activity across participants, we normalized EMG data based on our zero-impedance condition. Specifically, we averaged EMG data from all zero impedance trials for a given participant and took the maximum value from this averaged data for each limb muscle. We then divided all EMG data by this maximum value for each muscle and repeated this procedure for each participant [114]. We evaluated the participants' level of effort in hip abduction/adduction control during the stance phase by integrating EMG activity of GM muscles from 0-40% of the gait cycle [107]. In this study we focused on the analysis of the stance phase GM EMG activity because GM activity is the highest in stance phase for pelvic stabilization [82], [115]. We averaged the integrated EMG activity for the last 40 gait cycles from each impedance condition. We then averaged this number across the repetitions of impedance conditions so that each condition contained one averaged value for each participant and used later for statistical analysis. For the abduction and adduction assistance sessions, we performed one-way repeated measures ANOVA to determine if K-levels significantly influenced the step width or stance phase GM activity. p values less than 0.05 were interpreted as significant for all analyses. Post-hoc Tukey tests were performed if ANOVA analysis showed significance.

3.3 Results

3.3.1 Step Width and Step Length with a Steady K Value

Fig. 2 shows the influence of stiffness K of active hip exoskeleton abduction or adduction assistance on step width and step length. In average participants walked with wider steps during the abduction assistance session due to the applied abduction torque to both limbs over the whole gait cycle (Fig. 2(a)). The step width increased almost linearly (Pearson's $r = 0.665$, $p < 0.001$)

with the stiffness K in abduction assistance before saturation reached with K = 60 Nm/rad (i.e., participants produced the maximum step width). One-way ANOVA showed that change of K value in hip abduction significantly influences step width across participants, compared to ZI mode ($p < 0.001$). Furthermore, post-hoc Tukey tests showed that the average step width relevant to K = 20 condition was significantly smaller than the K = 60 and K = 80 levels ($p < 0.001$). Nevertheless, the calculated step length results did not show any statistical significance for various values of K, as shown

When the stiffness K of hip exoskeleton, acting in the adduction direction, increased, in average participants walked with narrower steps over the whole gait cycle as shown in Fig. 2(b). Due to the limited range of step width for human to walk with narrow width (compared to the range when walking wider), the step width hit the saturation value (smallest step width that human can walk comfortably) when K was only 20. Therefore, the step width did not reduce significantly when K was greater than 20. Nevertheless, statistical analysis revealed that, in comparison to walking in ZI mode (K = 0), in average participants walked with narrower steps with a stiffness

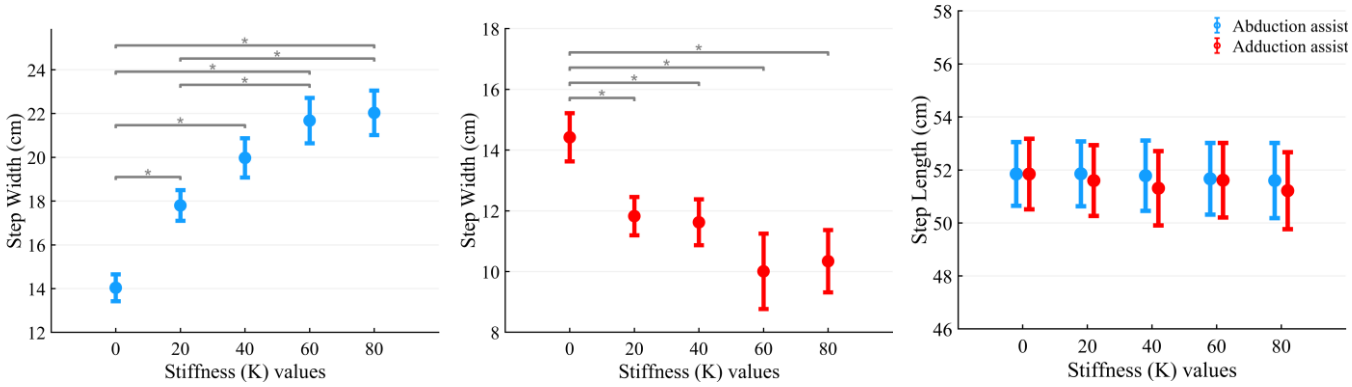

Figure 3.2. Influence of stiffness *K* of hip exoskeleton abduction (blue) and adduction (red) assistance on step width and step length. (a) Step width increased across *K* levels for abduction assistance mode. (b) Step width decreased across *K* levels for adduction assistance mode. (c) Step length did not change for the hip exoskeleton assistance regardless the assistance direction and applied stiffness. The data points represent the mean and error bars show the standard error mean, and asterisks (*) indicate significant ($p<0.05$) results of post-hoc tests.

value set more than zero ($p < 0.03$). Finally, similar to the step width increase session results, participants did not change their step length significantly for different stiffness K, as shown in Fig. 2(c)(red error bars).in Fig. 2(c)(blue error bars).

3.3.2 Transient Step Width Behavior

Fig. 3 shows the transient behavior of the participants in terms of the step width change at the moment of a stiffness change. Stiffness values were modified at the 20th heel strike in the figure. Normalized and averaged step width data across participants were shown for both abduction (Fig. 3(a)) and adduction (Fig. 3(b)) assistance when the stiffness K was changed from ZI mode ($K = 0$). As in Fig. 3, the step width reaction ocurred almost immediately after the stiffness changed. Using the CuSum method discussed in Appendix A, we quantified number of reactive heel strikes when stiffness K changed from 0 to other studied levels (Fig. 4). In general, when stiffness K increased from the zero, it only took less or equal to 4 strikes in the transient reaction for step width to reach steady state value. Note that we only focused on the stiffness change from $K = 0$ because the step width showed significant difference in steady state when K increased from 0 in this study (Fig. 2(a) and (b)).

3.3.3 GM EMG Activity

The GM activity did not vary significantly with abduction and adduction assistance over changed stiffness levels for both limbs. Fig. 5 shows the averaged pattern of the gluteus medius activity for all participants during abduction or adduction assistance. Only the left side is shown as an example. Table I summarizes bilateral integrated GM during the stance phase. Both results showed that no significant change of GM activation pattern was identified across studied K-Level conditions for either abduction or adduction assistance.

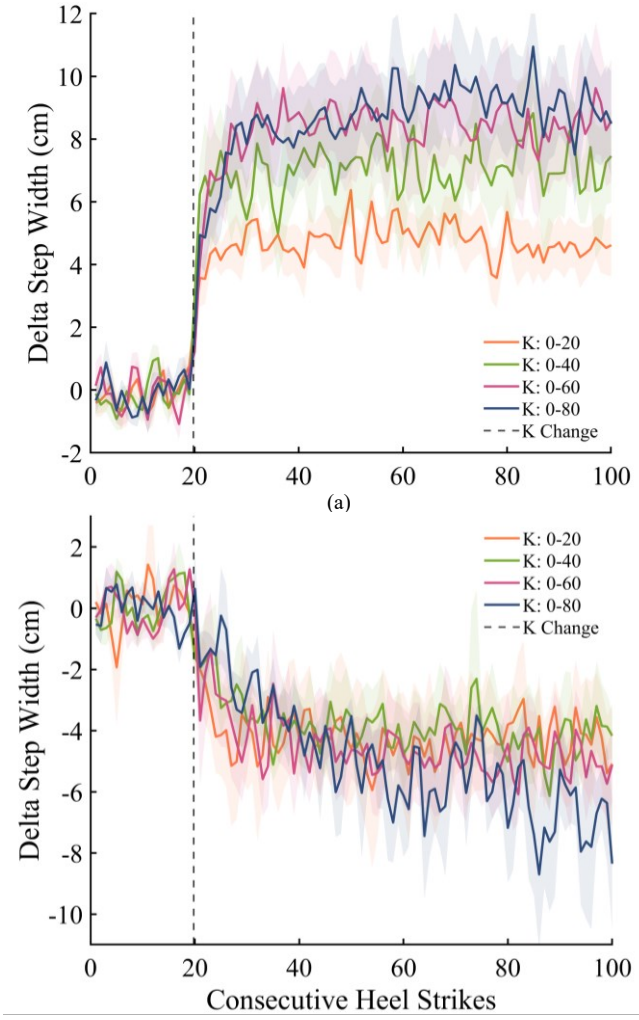

Figure 3.3. Transient behavior of normalized step width across changes of stiffness *K* from ZI model for (a) abduction and (b) adduction assistance.

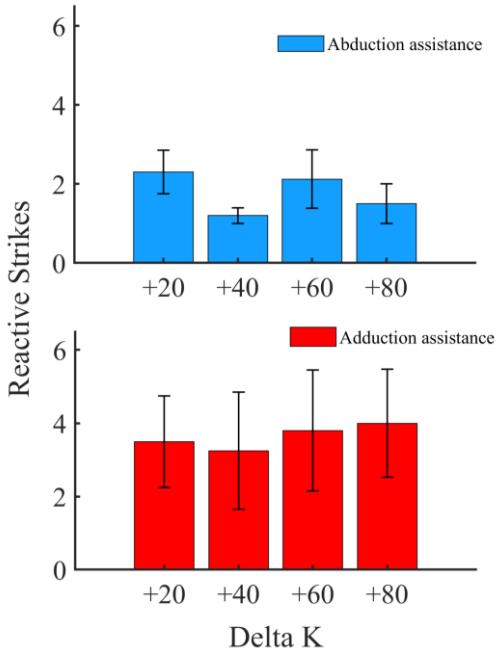

Figure 3.4. Transient responses of participants' step width to modulated stiffness levels is shown for Abduction assistance and Adduction assistance. Error bars represent the standard error mean.

3.4 Discussion

In this study, we presented a novel way to modulate human step width during normal walking via a hip exoskeleton, powering abduction/adduction by admittance control. Our hip exoskeleton application is fundamentally different from existing exoskeleton design and control. The vast majority of existing exoskeletons have been focused on assisting sagittal plane motions for cyclic stepping [99], [116]–[118], while ML balance is ensured by human users (e.g., using

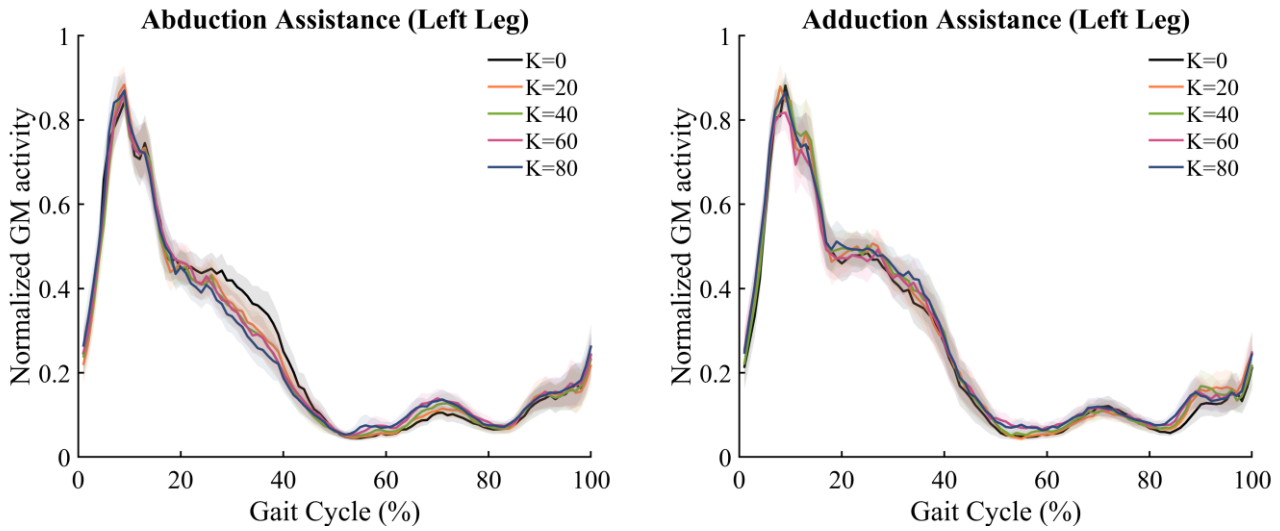

Figure 3.5. Modulated step width did not influence the activity of the *gluteus medius*. The average pattern of left leg GM for (a) abduction and (b) adduction assistance modes are plotted from heel-strike to heel-strike across all participants.

crutches) [119]. Although very limited studies have tried to use exoskeletons to react to a balance perturbation (i.e., control after a perturbation occurs), to our knowledge, no wearable robot approach yet exists to proactively modulate the step width for enhanced ML walking stability. Hence, in this study, we not only presented a new configuration and control of a bilateral hip exoskeleton, potentially for proactive ML balance augmentation, but also contributed new knowledge that adjusting the stiffness in the abduction/adduction admittance control of a hip exoskeleton can successfully modulate the human user's step width without influencing the step length during normal walking. This result implies that stiffness tuning can be a viable option for controlling step width, instead of relying on torque-tracking approaches that require a high-level torque reference command. In this study, we examined how humans respond to varied hip exoskeleton control parameters applied in ML direction. We observed an almost linear trend between altered stiffness and average step width for abduction until the step width reached a limit. Such a linear response in step width enables design of simple, linear controllers for closed-loop

TABLE I
RESULTS OF NORMALIZED STANCE PHASE GM EMG ACTIVITY

Limb	K	Abduction session stance phase norm. GM activity		K effect	Adduction session stance phase norm. GM activity		K effect
		mean	±SE		mean	±SE	
Left	0	0.49	0.03		0.5	0.04	
	20	0.47	0.03		0.52	0.03	
	40	0.46	0.03	***p = 0.96***	0.52	0.04	***p = 0.99***
	60	0.47	0.03		0.51	0.04	
	80	0.46	0.03		0.53	0.03	
Right	0	0.51	0.03		0.5	0.04	
	20	0.49	0.04		0.54	0.04	
	40	0.48	0.04	***p = 0.98***	0.53	0.04	***p = 0.98***
	60	0.49	0.04		0.52	0.04	
	80	0.48	0.04		0.54	0.04	

control of human step width via adjusting stiffness in admittance control during walking in the future [120]. Given that hip abduction/adduction assistance did not change the step length, the saturation of the step width was likely due to the biomechanical limits for participants to increase or decrease the step width with invariant step length during normal walking. Nevertheless, for adduction sessions, we did not clearly observe the linear relationship between stiffness K and step width. This is likely because the adjusting step of K-value (i.e., 20 Nm/rad) was too large while the biomechanical limit for reduced step width was small. A higher resolution of K-value change (e.g., increasing K by 5 Nm/rad increments) could potentially be used to further explore whether the control stiffness and step width maintains a linear relationship within the step width limit for hip adduction assistance. Finally, the average step length of the hip exoskeleton users did not change for either abduction or adduction assistance at various K levels, supporting previous studies that suggest independence between anterior-posterior and mediolateral foot placements [81]. These results suggest that separate controllers can be designed for 4 DOF hip exoskeletons controlling step width and length independently. Another factor that makes our presented approach for augmenting ML balance practical is that we did not observe gait disruptions (i.e., trips or use

of handlebars) among all participants during change of exoskeleton control K, even when the K value changed significantly (see supplementary video for reference). Such human response implied that we can adjust stiffness K during normal walking to achieve step width modulation safely. Participants smoothly adapted to the change in K and stabilized at the new step width within 4 strikes for both the abduction and adduction sessions. This response time may be inadequate to enable precise strike-to-strike step width control (or foot placement), which might be needed when walking on irregular ground surfaces, e.g., a rocky trail. Nevertheless, the response time is sufficient to proactively regulate the step width for enhanced ML balance during walking exercise. However, in this study, we only considered using stiffness K to change the step width. In addition, K value change is applied to the entire gait cycle. Further research is needed to understand if the ML hip exoskeleton can change step width within a single step by adjusting other admittance control values (such as equilibrium position), changing stiffness K only during a certain phase of the gait, or using closed-loop feedback control. The activity of GM during the abduction assistance indicated that increases in step width behavior were primarily due to changes in exoskeleton assistance level rather than changes in participant behavior. A previous study has demonstrated that volitional increases in step width are primarily generated by increased GM activity during the stance phase [107]. Nevertheless, our result indicated that, despite increased step width, GM activity did not change. This finding suggests that ML hip exoskeletons can provide assistive support for step width increase without imposing additional demand on the GM muscles. It also shows that ML hip exoskeleton's abduction assistance can be used with minimal resistance from non-disabled users. For the adduction assistance mode, GM activity did not change either. However, research showed that non-disabled individuals walking with narrower steps decreases EMG of GM . This finding suggests that hip exoskeleton users may resist narrowed step width.

This is potentially caused by perceived threat to their balance due to reduced base of support in ML direction and potential tripping by their own limb. To further investigate the cause of this resistive response to exoskeleton abduction torque, we might need to systematically examine the human user's subjective response on the sense of efforts and balance confidence. The presented hip exoskeleton, control, and human response may lead to many exciting applications. First, our exoskeleton design and study results could likely be utilized to enhance ML balance control in populations with declined sensorimotor functions or hip muscle weaknesses, such as post-stroke patients [121], older adults [122], or individuals with transfemoral amputations [123], [124]. It is essential to emphasize that the structure of our hip exoskeleton enables the implementation of alternative control schemes, offering flexibility in adjusting control parameters and their timing. Additionally, the capability to control the motors unilaterally presents a potential opportunity to address the asymmetrical gait observed in certain populations mentioned earlier. Our hip exoskeleton may also be used as an assistive or therapeutic device during their gait training in clinics or home in the future to address their walking balance. The proposed hip exoskeleton and control can be employed as a research platform to study ML balance control mechanisms. As a research tool, it can be used to further study the connection between step width modulation and balance to better comprehend the neuromechanical aspects of motion control during walking [125] inside or outside of the lab environments. These will be our future research directions. Finally, besides the limitations and future research discussed above, other limitations were also identified in our presented study. First, we carried out the study on a treadmill with a fixed speed and lab environment. It would be interesting to test the human response when walking speed varies or over level ground. In addition, the research focuses on human response in step width, step length, and GM activity only, we did not measure other biomechanics parameters in gait, such kinematics and

kinetics of knee and ankle. Further investigations are required to test additional muscle groups, in addition to the gluteus medius, to determine whether compensation by other muscle groups has occurred or not. More systematic analysis of human biomechanics while using our hip exoskeletons is needed in the future.

3.5 Conclusion

In this study, we successfully demonstrated the ability of our hip exoskeleton and its admittance control acting in the mediolateral direction to modulate step width in non-disabled participants. We showed that the step width of the users can be directly modulated by changing the admittance control parameters, namely stiffness K, once the added torque direction (either abduction or adduction) was defined by fixing the equilibrium angle (θeq) in the controller. After the stiffness K increased from zero to a studied value, we found that human participants started to react immediately after a K change and showed significant step width change within 4 strikes. In addition, besides the change of step width, the immediate stiffness change did not disrupt the gait and step length. When examining the activity of bilateral gluteus medius, which plays an important role for ML stability in gait, we found the activity does not show significant difference regardless of the level of stiffness value (and therefore torque applied). This observation indicated that the increase in step width was caused mainly by the exoskeleton rather than human efforts. This study outcome may pave a new way for designing closed-loop control of step width and foot placement in ML directions via our hip exoskeleton for assistive or rehabilitation purposes in the future.

CHAPTER 4

A. Alili, V. Nalam, Joshua R. Tacca, M. Liu, J. Si and H. Huang, Towards Advancing Mediolateral Balance by Hip Exoskeletons: A Reinforcement Learning-Based Approach for Proactive Step Width Control" in IEEE Transactions on Robotics, to be submitted

4.1 Introduction

Over the past two decades, numerous researchers have developed lower-limb exoskeletons for rehabilitation purposes and assistance with daily activities [126], [127]. Most exoskeletons, whether research prototypes or commercial devices, primarily provide power in the sagittal plane to facilitate cyclic steps during locomotion. However, these devices often overlook the requirement for mediolateral (ML) balance [119]. For instance, exoskeleton users with balance challenges will need to use crutches or canes to maintain balance in an upright posture.

Recently, there has been growing interest in developing exoskeletons that support balance during walking, particularly in the mediolateral (ML) direction. This is because maintaining ML balance requires more intricate active motor control, as the frontal plane poses greater challenges to stability [128][129]. Based on human biomechanics, Reimann et al. [80] demonstrated that the central nervous system primarily employs several key control strategies to ensure walking stability. Two strategies are directly related to lower limb joints. The first is the lateral ankle strategy, which manages small shifts in the center of pressure (CoP) to make relatively minor adjustments to balance during walking. From a wearable technology perspective, we are unaware of research attempts to improve ML balance using ankle exoskeletons due to the challenge of designing these devices without adding excessive distal weight. The second strategy is the

stepping strategy, which involves step width control in the ML direction and relies on the function of the hip joints. This strategy is considered as the primary method for maintaining ML balance during gait. This approach involves modulating the relationship between the ML position of the Center of Mass (CoM) and the Base of Support (BoS) to prevent instability during the single-limb support phase [130], achievable through step width adjustments [131] [82]. In addition, a study has showed that step width modulation directly influences ML balance by affecting frontal-plane external moments and whole-body angular momentum [132].

Since the hip joints play a crucial role in ML gait stability [80], [133] and adding weight close to the center of mass minimizes destabilizing effects, designing hip exoskeletons to facilitate ML balance is a more practical approach. As a result, emerging research efforts have begun designing hip exoskeletons that can power hip abduction/adduction to address ML balance control in recent years. Often, four degree-of-freedom (DOF) hip exoskeletons powered by series elastic motor [102] [134], cable-driven emulator [135], quasi-direct drive actuators [136], or harmonic gear driven actuators with active torque feedback with admittance control capabilities was designed [137]. Recent two studies [135] [136] applied on-off torque control (i.e., square wave) to 4-DOF hip exoskeletons to examine their effects on foot stepping in the frontal and sagittal planes following a balance perturbation.

These studies, however, did not use the balance related measures as feedback to perform closed-loop control. Very few have utilized the extrapolated center of mass (XCoM) as a metric to receive the balance feedback in both anteroposterior (AP) and ML direction to control the robotic exoskeleton [101], [134]. Wang et al. [134] used position control as the low-level control, while Zhang et al. [102] used admittance control. For both studies, the authors monitored the XCoM in ML direction. When it is outside of the bound after a perturbation, the control of hip

abduction and adduction will be activated and continuously regulate XCoM back in the stability bound.

All of this prior research, however, focuses on reactive approaches that intervene in the ML balance of exoskeleton users only after a shift in balance is detected, typically in response to perturbations. However, such solutions can be abrupt, jerky and address only the effects, not the causes, of balance loss. In contrast, *proactive* approaches aim to continuously adjust gait behavior to enhance the underlying mechanisms of balance, thereby improving overall walking stability and helping users to maintain balance against perturbations. The proactive approach may be a more effective path toward achieving continuous ML balance control. Additionally, studies aimed at improving ML balance with hip exoskeletons have mainly been conducted on a limited number of non-disabled participants as a proof of concept. Using hip exoskeletons to facilitate ML balance would be more appealing and useful to individuals with a hip weakness or impairment, including individuals with lower-limb amputations [138], post-stroke patients [139], or older adults [130]. For example, a transfemoral amputation leads reduced biomechanical function of biarticular muscles across the thigh and lead to weakened hip joint on the amputated side. They face unique challenges in maintaining ML balance and increase their vulnerability to ML instability [140].

Given the gaps in the field, our research goal has been to develop a modular hip exoskeleton and a control framework capable of proactively assisting the primary ML balancing strategy during walking. Unlike conventional exoskeletons, which primarily address AP stability or add ML support as a secondary feature, we developed a bilateral ML hip exoskeleton and validated its ability to deliver the torque necessary for step width alteration [137]. We found an approximate linear relationship between hip abduction/adduction stiffness adjustment and step

width, which is consistent with the conclusion of a prior biomechanical study [141]. That means we can model the human and exoskeleton acting on it as a linear system and potentially design a simple linear control, such as PID, to control the step width in a closed loop, as shown in our feasibility study on one non-disabled participant [142]. However, several key challenges still remain. (1) How to design the hip exoskeleton control in the frontal plane to control the step width accurately without losing the human-like step-to-step variability in walking? (2) How can the control adapt individual variations, particularly in users with motor deficits? This is because the model of the relationship between hip impedance and step width is not generalizable across individuals. The PID control parameters must be personalized. (3) How can we make step width control setup time efficient and practical for clinical use? That is to say, the amount of time required for personalizing the controller with human-in-the-loop cannot be too long. (4) Can the proposed adaptive controller be applied to diverse populations?

We addressed these challenges in this study by proposing a novel reinforcement learning (RL)-based optimal adaptive control (Fig. 1) for a hip exoskeleton (powered in ML direction) to control step width. The control has 3 levels. The low-level admittance control ensures human safety and allows step width variability in walking. The middle level control is the closed-loop PID control. By assuming our system is linear we employed a linear controller to continuously adjust hip stiffness to control step width in a whole gait cycle. The high-level control is RL that adaptively tunes PID gains, assuring accurate step width control. The high-level controller was implemented as a hybrid offline-online learning. The offline learning generates close to optimal policy based on the approximated linear model. The online learning finetunes the policy, if needed, with human-in the loop (HIL) optimization. The hybrid learning improves the time efficiency and reduces human effort in finding the robust PID tuning policy. Finally, the learning

policy was directly deployed to adapt PID control parameters continuously to produce desired step width in walking.

By integrating insights in biomechanics and human-exoskeleton interactions, application-specific hardware, and a novel optimal adaptive exoskeleton control framework, we validate our novel system to show that proactively controls step width accurately without losing natural human variability in walking is feasible in both able-bodied individuals and those with lower limb amputations, who requires hip assistances and ML balance support. The key contributions of this study are: 1) a novel system enabling precise, proactive step width control in both non-disabled individuals and individuals with lower limb amputations, which to our knowledge has not been demonstrated previously; 2) a control framework that permits safe user overrides and interactions and exhibits robustness to external disturbances; 3) an effective learning paradigm that required only a single real-time HIL episode to fine-tune the offline-trained RL policy; and 4) a new evidence that step width control in hip exoskeleton users does not increase step width variability, confirming the absence of adverse balance interventions.

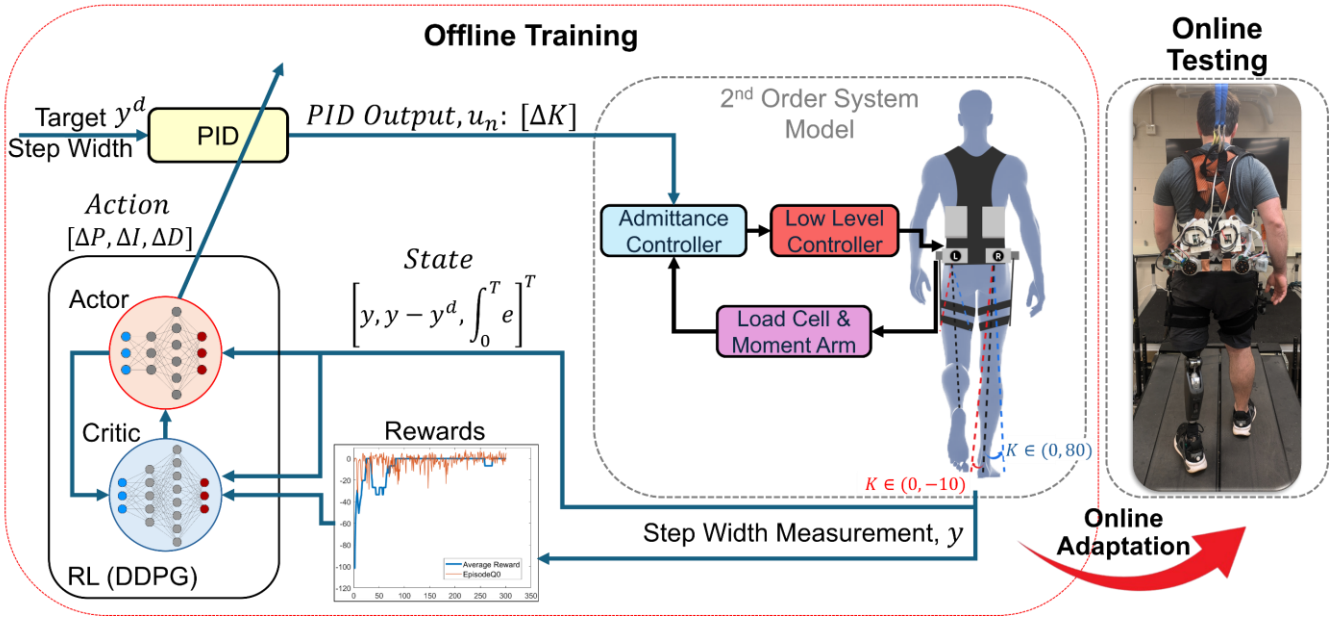

Figure 4.1. Step width control framework consisting of two phases: Offline Training of the RL Agent and Online Testing. The RL agent is trained offline based on the 2nd-order state-space human-exoskeleton model. The performance of the trained agent is then adapted in real-world settings to control the step width of robotic hip exoskeleton users.

4.2 Methods

4.2.1 ML Hip Exoskeleton and Control Implementation

A 2-DOF powered and compliant robotic hip exoskeleton, developed by the Neuromuscular Rehabilitation Engineering Laboratory (NREL) [137], was used in this study. The design incorporated a modular motor controlled by an admittance controller. The device featured two Maxon brushless EC flat motors (Taunton, MA, USA) operating in the frontal plane, with passive hinges allowing sagittal plane movement. It included a harmonic gearbox (CSD-20-100-2A-GR-SP674, Harmonic Drive) with a 100:1 transmission ratio, delivering 34 Nm of torque and up to 57 Nm at peak. Hip abduction/adduction angles were measured by a Maxon encoder, and interaction torque was captured via a load cell on the actuator arm. The exoskeleton was secured around the waist and thighs using cuffs.

To ensure safe and compliant interaction between the exoskeleton and the user, we applied admittance control [105] to power hip abduction/adduction. The admittance controllers used virtual impedance parameters—stiffness (K), damping (B), equilibrium angle (θ_{eq}), and inertia (M)—to model the human-exoskeleton dynamics. Based on the observed interaction torque (τ_{int}), admittance control determined the angular velocity reference for the low-level controller to generate the necessary motor torque, following the dynamics in Equation 1. Real-time control was executed via EtherCAT (TwinCAT 3.1) at 1000 Hz.

$$\tau_{int}(t) = M\ddot{\theta}(t) + B\dot{\theta}(t) + K[\theta(t) - \theta_{eq}] \tag{5.1}$$

The equilibrium angle (θ_{eq}) was held at +15° for the entire experiment. It allowed for an increase in step width by setting positive stiffness values, while decreasing it by applying negative values [143]. We used the stiffness (K) parameter to control step width throughout the gait cycle, while M and B were fixed at 0.2 and 0.7, respectively, from prior tuning. In zero impedance (ZI) mode, where $K = 0$, the exoskeleton matches hip movement without applying any torque. For step width control, we used positive values of K to increase the step width and negative values to decrease it. Thus, the K parameter range was set between -10 and 80 Nm/rad [142], [144].

4.2.2 General Framework for Step Width Control and RL-Based Learning

In our previous study, we performed a preliminary analysis to verify if PID control can be utilized to regulate step width [142]. To achieve control, we modeled the human-exoskeleton system as a combination of two second-order models that represent the relationship between stiffness and step width, each for modeling abduction and adduction behavior. System identification methods were used to identify the parameters of this second order system. Appropriate PID controllers were then tuned manually for abduction/adduction control.

However, manual tuning is empirical, tedious and non-optimal. To ensure optimal step width performance, we develop an RL based approach. The second order model used for step width abduction control was employed in this study to train a RL algorithm to tune the PID gains offline and test its validity in real settings (Fig. 1**)**. The low level PID controller was designed to modulate stiffness within a range of positive and negative values to increase and decrease step width, respectively. During real time testing, the PID control was executed at 50 Hz to modulate step width. We added noise to the offline measurement of the step width to emulate the real behavior of the step width variability.

The developed RL framework iteratively updates the PID gains so that the stiffness is optimally and rapidly modulated to control the step width of users. Our objective was to pretrain a single policy capable of adapting to various users. This is achieved by offline training on the second order models, where the PID gains were updated every two seconds for each step, with a randomly generated target step width that remained constant throughout the same episode. All PID gains were also randomized at the start of the episode until the RL algorithm determined the first set of values, enhancing the robustness of the training process.

The step width control state variables $\mu \in R^3$ for the RL are defined as the measured step width (y), difference between measured and target step width (y^d) and the accumulation of the error initialized to zero at each RL update:

$$\mathrm{S} = \left[y, e, \int e\right]^T \tag{5.2}$$

where $e = y - y^d$. Meanwhile, action variables $a \in R^3$ are defined in the following form:

$$A = [\Delta P, \Delta I, \Delta D]^T \tag{5.3}$$

where ΔP,ΔI,ΔD are adjustments of the PID gains for the corresponding time step of RL training.

The reward value in each update step, m, was calculated as follows:

$$r_m = r_1 + r_2 + r_3 + P = -\alpha_1 * \left(\frac{|e|}{Max\ Error}\right)^2 - \alpha_2 * \left(\frac{\int_m^{m+2}|e|}{Max\ Integral\ Error}\right)^2 - \alpha_3 * \left(\frac{\left|\frac{du}{dt}\right|}{Max\ Error}\right)^2 - P \quad (5.4)$$

$$P = \begin{cases} 100 & if\ y < 5\ or\ y > 40 \\ 0 & else \end{cases}$$

where $\alpha_1, \alpha_2, \alpha_3$ are weights equal to 1, 0.7 and 0.4, respectively. We designed the reward functions in a quadratic form, where the r_1 term ensured the elimination of steady-state error, and the r_2 term encouraged the model to reach a new steady state as quickly as possible. To provide a comfortable user experience, we included an r_3 term that discouraged abrupt changes in PID output. Additionally, we implemented measures to maintain realistic step widths by applying a strict penalty if the width exceeded 40 cm or dropped below 5 cm, as reflected in the final term in Equation (5.4).

The Deep Deterministic Policy Gradient (DDPG) reinforcement learning algorithm [145] was used for training. The DDPG algorithm consists of an agent with an actor, which takes an input state vector, $\mu(S)$, to produce an action vector, A, and a critic, an artificial neural network (ANN), which takes both the state and action vectors, $Q(S, A)$, to estimate the long-term discounted reward based on the Bellman equation. Both the actor and critic networks were designed and trained using the Reinforcement Learning Toolbox in MATLAB 2024a (MathWorks, USA).

The state input of the critic network consisted of an input layer with 3 nodes for the state input, followed by fully connected layers with 250 hidden neurons. These were followed by batch normalization and rectified linear unit (ReLU) layers for nonlinear transformation, and then by a second fully connected layer. The action input of the critic contained the action space, followed by a fully connected layer with 250 hidden neurons. These two paths were added together and passed through another set of batch normalization and ReLU layers, finishing with a fully connected layer.

The actor network, in turn, started with the state input, followed by two fully connected layers, each with 250 neurons, along with ReLU and batch normalization layers. These layers applied transformations to the state input, enabling nonlinear behavior in the actor network. The action output consisted of a fully connected layer followed by a *tanh* activation function to ensure that the action output was between -1 and 1. A scaling layer then transformed the output by applying predefined scaling factors. The hyperparameters of DDP and PID are shown in Table I.

At the beginning of the initial training process, the weights of the actor and critic networks, μ and Q, were randomly initialized. A target actor and target critic network, μ' and Q', were also created with identical structures and with weights θ^Q and θ^μ. The training consisted of 1,000 episodes. At the start of each episode, a new randomly generated target step width from a realistic step width range was selected, and the PID gains were randomly initialized. Each episode included a fixed number of 20 update steps. During each episode, the training process cycled through each data set using the current PID gains, selecting a new data set for each update step. At the start of each update step, the PID gains and measured step width data for the next data cycle were loaded. Step width for the data cycle were then obtained from the 2nd order abduction model. For update step m, the state vector, S_m, was calculated and the current reward, r_m, was determined using (4).

The action vector, A_m, was then obtained from the actor network according to the following process:

$$A_m = \mu(S_m) + N_m. \tag{5.5}$$

Here, N_m represents a noise vector sampled from an Ornstein-Uhlenbeck (OU) process [145], which facilitates exploration during training. The next cycle of data for the was then loaded and a new state vector, S_{m+1}, was calculated from the resulting step width calculated from the 2nd order human-exoskeleton model. A transition, defined as (S_m, A_m, r_m, S_{m+1}), was stored in a first-in-first-out buffer, D. Following this, to update the weights of the networks, a minibatch containing N transitions randomly sampled from D was obtained. The weights of the critic were first updated by backpropagation to minimize the loss function:

$$L_Q = \frac{1}{N}\sum_i (y_i - Q(s_i, a_i|\theta^Q))^2 \tag{5.6}$$

where y_i is a target value based on the Bellman equation and defined as:

$$y_i = r_i + \gamma Q'(S_{i+1}, \mu'(S_{i+1})), \tag{5.7}$$

γ represents the discount factor. The actor's weights were then updated via backpropagation to maximize the long-term discounted reward, as estimated by the critic network, through optimizing the policy gradient:

$$\nabla_{\theta^\mu} J = \frac{1}{N}\sum_i \nabla_{\mathrm{A}}\, Q\big(S_i, \mu(S_i)\big)\nabla_{\theta^\mu}\mu(S_i) \tag{5.8}$$

Finally, the weights of the target actor and critic networks were updated by:

$$\begin{aligned} \theta^{Q'} &= \tau\theta^Q + (1-\tau)\theta^{Q'} \\ \theta^{\mu'} &= \tau\theta^\mu + (1-\tau)\theta^{\mu'} \end{aligned} \tag{9}$$

where $\theta^{Q'}$ and $\theta^{\mu'}$ are the weights of target actor and targe critic. The hyperparameters of the DDPG used in this study are listed in Table I.

Training of the RL DDPG model was stopped once convergence in performance was detected. A small value of -0.01 was set as the convergence criterion, based on the average reward value over a window of 15 steps.

TABLE I
HYPERPARAMETERS OF DDPG RL AND PID

Hyperparameters	**Value**
Discount factor	0.97
Batch size	16
Experience buffer length	4000
Target smooth factor	0.001
Actor learning rate	0.001
Critic learning rate	0.001
Gradient thresholds	1
Noise Variance	0.3
Noise Variance Decay rate	0.0001
Execution environment	GPU
Action range for K_p	(-10, 10)
Action range for K_I	(-150, 150)
Action range for K_D	(-1, 1)
PID Output Range	(-10, 80)

4.2.3 Experimental Protocol

Our primary goal was to evaluate the RL performance during validation tests with hip exoskeleton users walking on a treadmill. The experiment was conducted in a single day and divided into four main sessions: 1) determining the participants' preferred treadmill walking speed, 2) identifying the step width range of hip exoskeleton users with maximum and minimum stiffness, 3) retraining the RL agent, which was initially trained offline, and 4) conducting two validation trials.

To ensure efficient human-device interaction, participants first walked for 3 minutes on the treadmill with the hip exoskeleton in zero impedance (ZI) mode at their self-selected walking speed [146].

Before proceeding to the real-time RL agent retraining session, we measured the whole gait low-pass filtered step widths using a moving average for three conditions: walking with a normal step width, the widest step width with maximum stiffness applied (80 Nm/rad), and the narrowest step width with minimum stiffness applied (-10 Nm/rad). The goal of this session was twofold: 1) to determine the step width range to ensure appropriate target step widths are randomly generated during real-time retraining, and 2) to prepare for validation trials by selecting the target step width.

Afterward, we conducted real-time human-in-the-loop (HIL) optimization to retrain the RL agent, allowing the model to fine-tune if necessary and to measure the number of episodes required for convergence. Unlike the offline training, we relaxed the convergence criterion from -0.01 to -0.1. If convergence was not achieved, the agent's retraining would be stopped after five trials, each lasting 3 minutes of participant’s walking on the treadmill.

To assess the performance of the proposed framework for controlling the step width of hip exoskeleton users, we designed two validation trials. The first validation trial aimed to test the behavior of the proposed controllers with respect to step inputs as the target step width. For each participant, three step inputs were set: one higher than their normal step width, followed by one lower, and another higher again. These target step widths were randomized across participants. The second validation trial aimed to test the robustness of the proposed framework against user-induced disturbances. At the end of each 60-second interval, an auditory cue prompted participants to voluntarily alter their gait by decreasing and increasing their step width for one step and stopping

the resistance. This test assessed whether the control framework could handle disturbances caused by user behavior. Overall, this session allowed us to evaluate the controller's effectiveness in controlling the step width of hip exoskeleton users.

4.3 Experimental Validation

4.3.1 Participants

Eight participants (five non-disabled, two with transfemoral, and one with transtibial amputations) took part in this study. To effectively demonstrate the step width control performance of the proposed framework, we selected a diverse group of participants based on factors such as age, height, sex, walking speed, prior experience with hip exoskeletons, and disability level. The details are listed in Table II. The study was conducted with approval from the Institutional Review Board of the University of North Carolina at Chapel Hill (13-3028), and all participants provided informed consent.

TABLE II
DEMOGRAPHIC AND PARTICIPANT CHARACTERISTICS

Participants	Sex (Male, Female)	Age (years)	Height (m)	Weight (kg)	Walking Speed (m/s)	Experience Level (#of times used before)	Physical Condition
1. AB01	M	20	1.73	80.7	0.8	1	Non-disabled
2. AB02	M	35	1.7	64.1	0.9	25	Non-disabled
3. AB03	F	19	1.73	60.8	0.8	0	Non-disabled
4. AB04	M	21	1.85	77.1	0.9	0	Non-disabled
5. AB05	F	20	1.65	63.5	0.95	3	Non-disabled
6. TFA01	M	45	1.73	74.8	0.5	5	Transfemoral Amputee
7. TFA02	M	26	1.68	83.9	0.65	8	Transfemoral Amputee
8. TTA01	M	57	1.75	109.8	0.8	0	Transtibial Amputee
Mean±Std		30.4±14.1	1.72±6.1	76.8±15.8	0.78±0.15	5.2±8.5	

4.3.2 Experimental Setup

A 12-camera motion capture system (VICON, Oxford, UK) sampled at 100 Hz was used to track participants' foot movements as they walked on an instrumented split-belt treadmill (Bertec

Corp., Columbus, OH, USA). Five reflective markers were placed on each foot—on the second toe, posterior heel, fifth metatarsal head, and lateral and medial malleoli—to capture foot movements. Ground reaction forces (GRFs) were measured by the treadmill, which was synchronized with the motion capture system and recorded at 1000 Hz.

4.3.3 Data Processing, Evaluation Metrics, and Statistics

Marker positions were low-pass filtered using a fourth-order Butterworth filter with a 10 Hz cutoff frequency, while GRF signals were filtered with a 25 Hz cutoff. Heel strike events were identified based on the GRF of each limb, using a 30 N threshold [111]. Step width was calculated as the mediolateral distance between heel markers at each heel strike [107]. For the steady-state response calculation, step width was calculated using the last 60 heel strikes (30 gait cycles) before the next transition. For both validation trials, the average step width for each participant was calculated along with step width variability, which was defined as the standard deviation from the last 60 steady state steps.

In addition to the steady-state response, we were also interested in the transient behavior of the controlled signal. Transient behavior was defined as the number of steps required to reach the range of the mean ± standard deviation of the steady-state condition. The number of steps was calculated from the step width measurements following either the step inputs or the perturbations introduced by the participants during the validation trials.

To test the significance of step width variability across the three phases of the first validation trial and the two phases of the second validation trial, we performed a one-way repeated measures ANOVA. This analysis aimed to determine whether the step width control trials had a significant effect on step width variability. A p-value of less than 0.05 was considered statistically significant for all analyses. If the ANOVA results indicated significance, post-hoc Tukey tests

were conducted. Bartlett's test was used to assess the homogeneity of variance, and the Lilliefors test was employed to evaluate the data normality.

4.4 Results

4.4.1 Offline and Online Convergence of the Framework

The RL training converged after 300 episodes during the offline learning phase, taking approximately 45 minutes with GPU support. Fig. 2(a) illustrates the learning behavior of the DDPG model in terms of the accumulated reward and Episode Q0, which represents the estimated discounted long-term reward at the start of each episode. For agents with a critic, this estimate is based on the initial observation of the environment. The offline learning of the RL agent automatically stopped when the convergence criterion of was met, based on the average reward value being less than -0.01 over a window of 15 steps. Fig. 2(b) shows the adaptively tuned PID to adjust the stiffness of the admittance controller for the last episode of learning, ensuring the step width reaches the defined target value (Fig. 2(c)).

We also tested the stability of the PID acting abduction model, which represents the mathematical relationship between modulated hip exoskeleton stiffness and human step width, used to train the RL agent for all combinations of the proposed PID gains. Fig. 3. shows the pole-zero map for the last training episode. As can be seen from the figure the stability was conserved for all 20 steps of PID gain updates.

As part of the experimental protocol, we retrained the RL agent, previously trained offline, to determine if further training was necessary. After just one episode, the RL model converged for all participants, demonstrating the robustness of the offline trained policy.

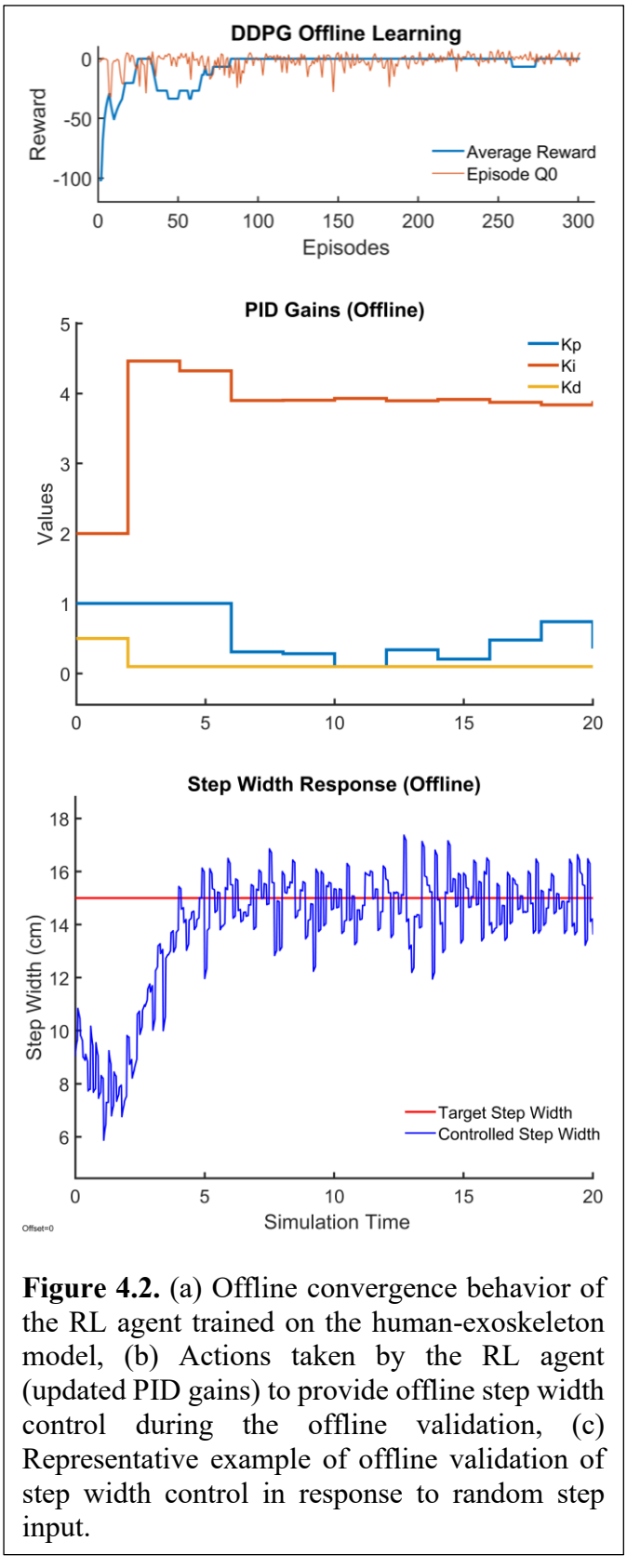

Figure 4.2. (a) Offline convergence behavior of the RL agent trained on the human-exoskeleton model, (b) Actions taken by the RL agent (updated PID gains) to provide offline step width control during the offline validation, (c) Representative example of offline validation of step width control in response to random step input.

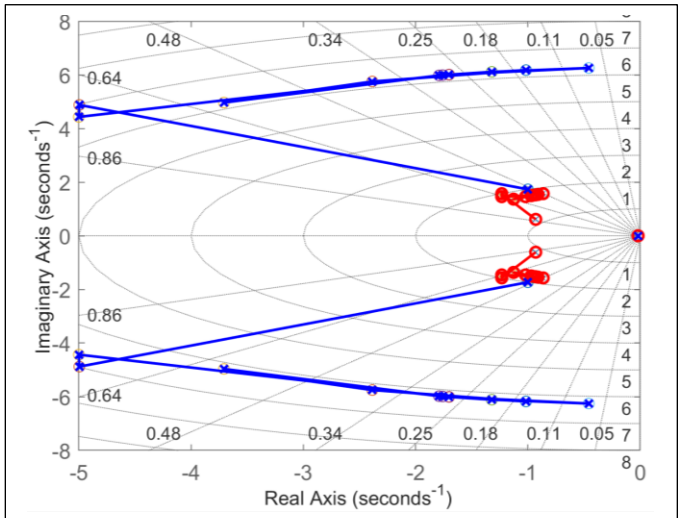

Figure 4.3. Pole-Zero Map demonstrating the stability of the 2nd-order state-space human-exoskeleton model controlled by an RL-tuned PID during representative offline validation. The map is depicted for each pair of adaptively adjusted PID gains. Blue crosses and red circles represent the evolution of poles and zeroes, respectively.

4.4.2 Transient control behavior

The primary goal of the study was to develop a framework that can adapt to the walking dynamics of various hip exoskeleton users and provide accurate control of step width.

Fig. 4. qualitatively displays the control of step width for first validation trial for participants TF01 and AB02. Fig. 4(a, b) shows the step width measured throughout the entire gait cycle at 100 Hz, which was low-pass filtered using a moving average. Fig. 4(c, d) represents the adaptive adjustment of the PID controller tuned by RL. Observations revealed that the generated PID gains used to control step width varied across participants, as evident in the cases of TF01 and AB02. On average, the difference between the controlled step width (measured at each heel strike during offline analysis) and the target step width during the first validation trial across participants was 0.51 ± 0.52 cm, 0.48 ± 0.4 cm, and 0.86 ± 0.52 cm in terms of mean and standard deviation for the three step inputs.

The transient behavior of step width control was another crucial point for our study, as our goal was to ensure a smooth transition with as few steps as possible. We achieved smoothness by incorporating a penalty in the reward function to avoid abrupt changes in the PID control signal. At the same time, rapid transitions were encouraged by rewarding the reduction in accumulated error. The number of steps needed to transition from wider to narrower and from narrower to wider conditions for the first validation trial, on average, was 5 steps and 4 steps, respectively.

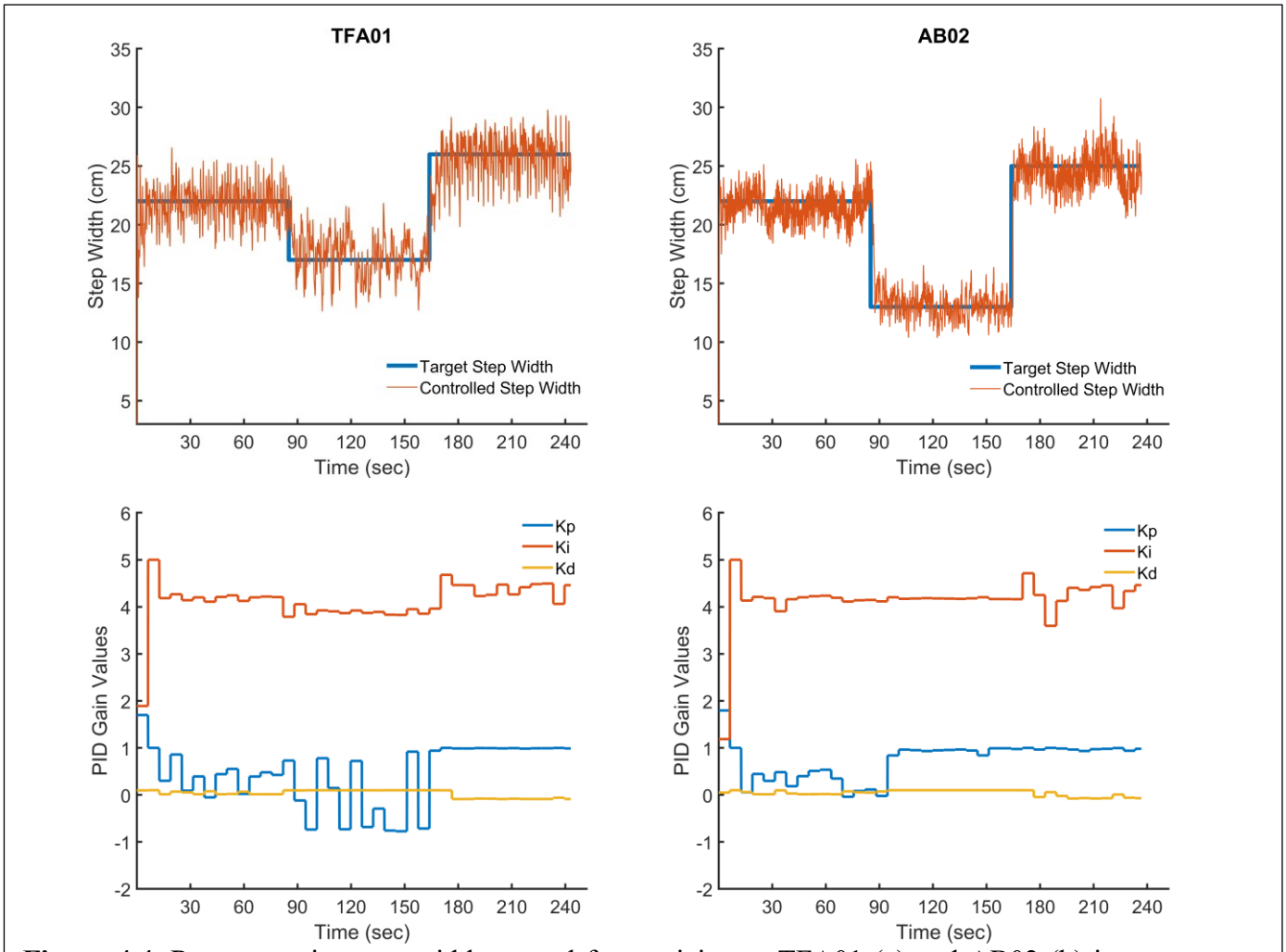

Figure 4.4. Representative step width control for participants TFA01 (a) and AB02 (b) in response to randomly generated target step widths. (c), (d) Adaptively adjusted PID gains by the RL agent to ensure step width control for the two participants.

4.4.3 Disturbance Rejection Behavior

Figs. 5, 6 illustrate the moments when TFA01 and AB02 overrode the hip exoskeleton's applied torque by voluntarily decreasing or increasing their step width. The step width control behavior for both participants is shown in Fig. 5 (a, b), while Fig. 5 (c, d) displays the PID controller output in response to the introduced disturbances. Notably, immediate reactions in the PID output can be observed around the 80th and 140th seconds.

For the second validation trial, the difference between the target and steady-state step width measurements at each heel strike over the last 60 steps following the disturbances was 1.11 ± 0.6

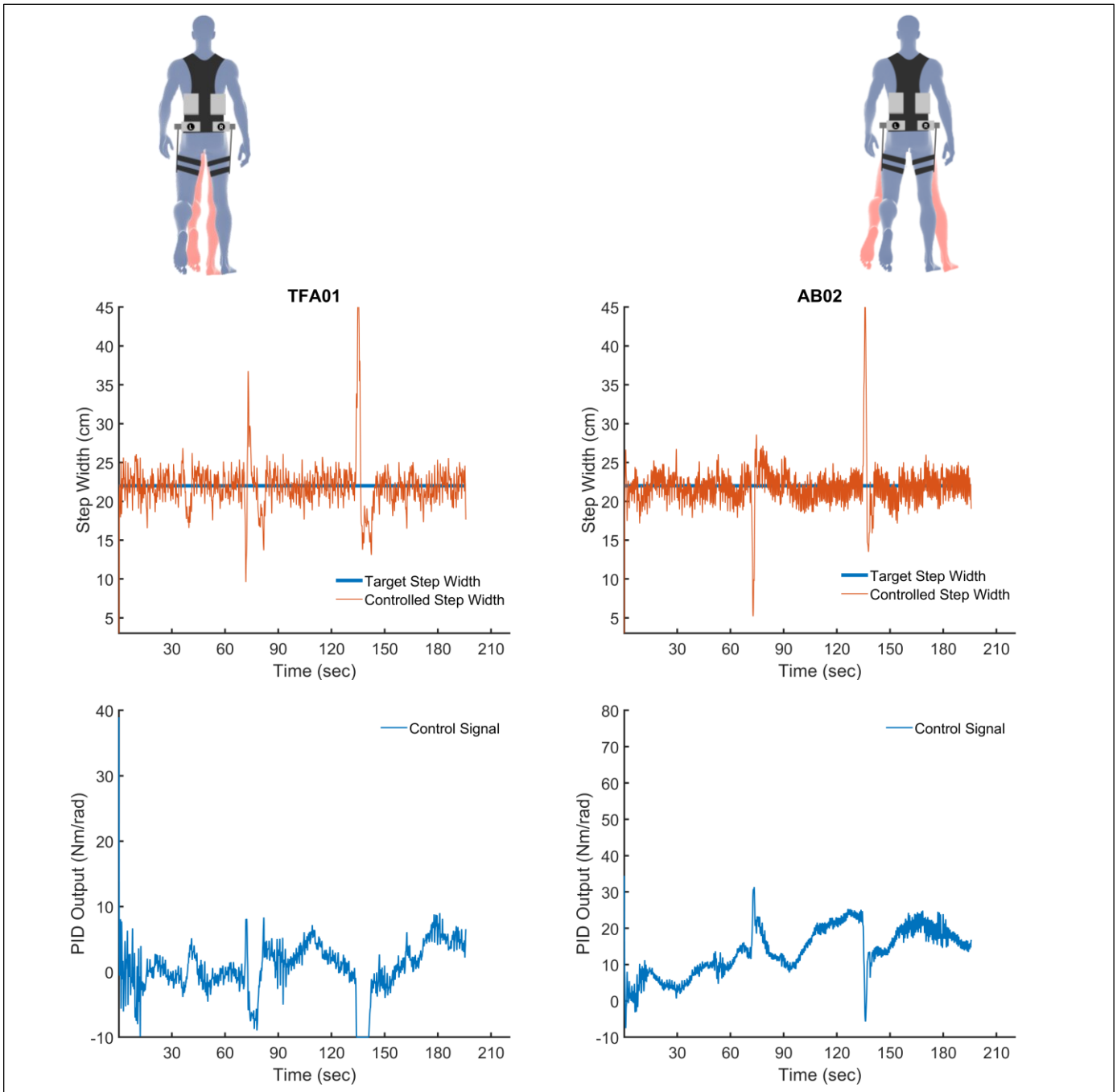

Figure. 4.5. Representative step width control for participants TFA01 (a) and AB02 (b) in response to volitional overrides of step width control following auditory cues. (c), (d) PID outputs showing the stiffness adjustments in response to user induced disturbances.

cm and 1.07 ± 0.44 cm, as shown in Fig. 6(a). Additionally, the median number of steps required for the framework to return participants' step width to the target after disturbances was 2 and 3, for the narrow and wide disturbances, respectively (Fig. 6(b)).

4.4.4 Step Width Variability

To control step width, we implemented an admittance control architecture for the low-level exoskeleton control. This architecture allowed for natural overrides when necessary, while preserving the natural step width variability introduced by the human user. Our goal was not to inhibit this variability, as it is closely related to human balance capabilities, as reported in [147], [148]. To assess this, we measured the steady-state step width variability among participants across both validation trials and their respective phases. The median step width variability ranged from 1.6 to 2.4 cm across the two trial phases. ANOVA tests showed no significance for step width variability among the phases of validation trials.

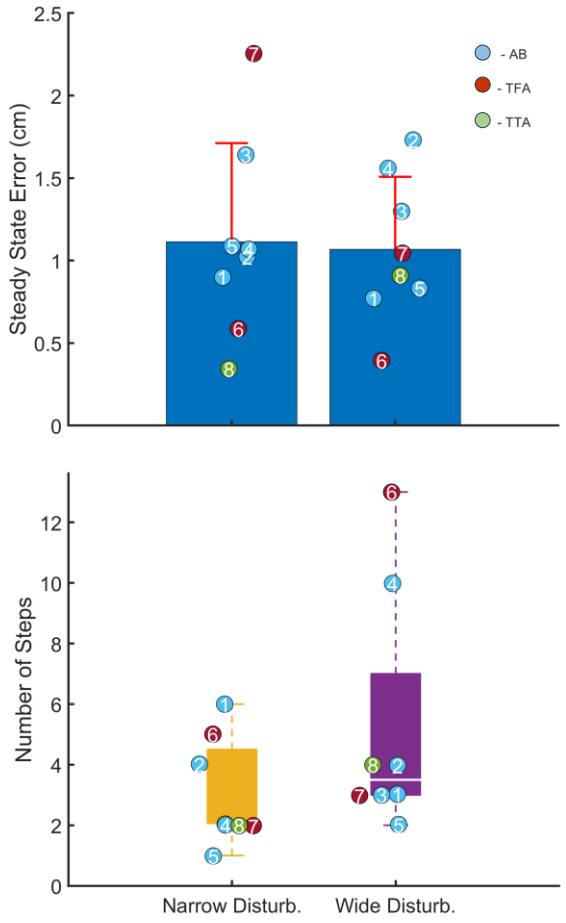

Figure 4.6. Bar plots depicting the mean and standard deviation across participants for the difference of controlled step width (averaged for the last 60 heel strikes) and the three target step widths across all participants. Numbers represent the participants.

4.5 Discussion

In this study, we introduced a novel framework that, to the best of our knowledge, is the first to efficiently adapt and accurately control the step width of users wearing a hip exoskeleton during normal walking. We employed a reinforcement learning (RL) algorithm to tune the PID gains, which govern the stiffness parameter of the admittance controller responsible for generating abduction/adduction torques applied to the hip. The RL policy was initially trained offline using a

mathematical model designed to capture the relationship between the modulated stiffness input and the step width output of a human wearing the exoskeleton. Subsequently, the RL policy was fine-tuned for each participant as they walked on a treadmill. Due to the robust representation of human dynamics in the mathematical model, which enabled effective offline RL training, and the well-structured Deep Deterministic Policy Gradient (DDPG) actor-critic networks, only a single real-time episode lasting for 3 minutes was needed to update the policy for each participant. This approach eliminated the need for prolonged and resource-intensive human-in-the-loop optimization trials. The time we achieved for online fine-tuning of the RL policy is among the shortest observed, especially when compared to the average time of 33 minutes typically required for human-in-the-loop optimization in wearable robotic devices with various objectives [149]. Furthermore, we demonstrated that well-designed mathematical models capturing human dynamics can be an effective choice for offline learning. The proposed framework's effectiveness was validated through its accurate control of step width and its ability to reject disturbances across participants with diverse demographic and physical characteristics.

We evaluated the steady-state accuracy of the proposed framework by setting three target step widths, updated every 90 seconds while continuous walking and randomized across participants. Each participant’s individual step width range, determined by the maximum applied abduction/adduction torque, was considered when selecting these target widths. On average, the difference between the target and real-time controlled step width, measured at each heel strike, was less than 1 cm across all participants for the three targets. Notably, the framework demonstrated consistent control accuracy, despite substantial differences in participants' lower-limb mechanics. In our previous study [150], we showed that modulating step width using a mediolaterally active hip exoskeleton can influence the gait balance in terms of ML net external

moment, the margin of stability, and trunk sway. Taken together, these findings and the level of precision achieved with the step width control reinforce the framework's potential to enhance gait balance in individuals with neuromechanical deficits or lower limb amputation.

The transient behavior of the developed framework was also of significant importance, in addition to its steady-state performance. We measured the number of steps required for the framework to bring each participant's step width to a new steady state during the first validation trial. On average, a median of five steps was needed to reach the new steady state, whether transitioning from a wider to a narrower step width or vice versa. As noted earlier, we deliberately prioritized smooth transitions while minimizing the number of steps required to reach a steady state, considering the participants' physical profiles. Additionally, we gathered participant feedback on their experience during these transitions. TFA01's brief response, "Smooth!", was echoed by other participants, who reported similar experiences. This achievement can facilitate the device acceptance process for daily use and contribute to shorter and more effective adaptation periods.

The second validation trial was designed to evaluate how effectively the developed framework handles user-induced disturbances. This trial had two primary objectives. First, we aimed to demonstrate that the proposed low-level architecture allows for easy user overrides, a feature deliberately integrated during the development of the hip exoskeleton [137]. This feature is particularly important for the population we aim to assist, including older adults, individuals with lower-limb amputations, and stroke patients, who retain a degree of gait independence. Therefore, it is essential that these users can control the device when necessary. The second objective was to show that the framework is robust in managing disturbances and capable of returning the users' step width to the predefined targets. The results demonstrated that all

participants were able to easily override the hip exoskeleton's control and adjust their step width in response to auditory cues. Similar to the first validation trial, the difference between the target and steady-state step width, measured at each heel strike, was less than 1 cm across all participants following both volitional decreases and increases in step width. While analyzing the transition behavior, we observed that one of the transfemoral amputee participants (TFA01) reacted very sensitively to the applied hip exoskeleton torque after overriding the device control (Fig. 5a). We presume that this heightened sensitivity to the corrective torque, applied to adjust step width to the target, may be due to hip weakness associated with limb loss. However, the average number of steps required for the framework to return the user's step width to the target was between 2 and 4. These findings further reinforce the potential application of the framework, especially considering that the number of steps required for non-disabled individuals to recover from perturbations is typically less than 6 [151], [152]. It is important to note that the rationale for using the RL-tuned PID for step width control, rather than allowing RL to directly tune the admittance control parameters, was to achieve faster response times.

As previously mentioned, step width variability is a commonly used metric to assess fall risk in older adults and clinical populations. To evaluate whether the framework introduced any additional noise to the participants' step width, we measured the controlled step width variability across all trials. The results showed that the step width variability of participants remained within the normal range of 2-3 cm, as reported in the literature [153]. This feature provides additional confidence in using the framework to positively influence the ML gait balance of hip exoskeleton users.

In addition to its significant potential for improving gait balance as an assistive technology, the proposed framework can also be used for rehabilitation purposes. Studies involving

flexion/extension robotic hip exoskeletons have shown positive outcomes in the rehabilitation of stroke survivors, older adults, and individuals with lower limb amputations, improving spatiotemporal gait symmetry, metabolic efficiency, and kinematic quality [154], [155]. Similarly, the framework can be used as a research tool to investigate stability-related step width control responses by applying ML perturbations, typically conducted using non-mobile systems [156], [157].

Along with achieved results our study presents a few limitations. First, the experiment was conducted on a treadmill with a fixed speed in a controlled lab setting. It would be valuable to explore how well the framework controls human step width when walking speeds vary or when walking occurs on level ground. Moreover, our research primarily focused on human responses in terms of step width. We did not account for other biomechanical parameters in gait, such as the kinematics and kinetics of the knee and ankle. Future research should measure lower limb muscles activity to assess whether compensation by other muscles occurs. A more comprehensive analysis of human biomechanics during the use of our hip exoskeleton is also required for future studies. In addition, human-machine adaptation over extended periods of time is an important area of interest for future studies. The next and most significant stage of this study will involve demonstrating the ML gait balance intervention for individuals with balance deficits, using step width control facilitated by a robotic hip exoskeleton.

CHAPTER 5

5.1 General Conclusion

This study presents significant advancements in the field of wearable robotics, specifically in lower-limb prosthetics and exoskeletons, by introducing novel control frameworks that prioritize user preferences and address gait balance. It highlights the importance of integrating user preferences into prosthetic control systems, leading to personalized assistance and improved usability. By incorporating reinforcement learning and admittance control, the research shows how robotic systems can enhance mobility and stability, particularly through the modulation of step width to improve gait balance, a critical concern for lower-limb amputees and individuals with compromised hip muscle function. These findings suggest promising applications in rehabilitation and daily use, with the potential to improve the quality of life for users by providing more intuitive, responsive, and effective robotic assistance.

5.2 Future Work

In future work, we will continue exploring various ways to advance wearable device control by incorporating user preferences and enhancing gait balance for wearers.

Regarding the user preferences study, further research is needed to assess the consistency of user preferences over extended periods. Future investigations should also include joint kinematics computation and EMG signal monitoring during biomechanical analyses. In our current study, participants could only modify control points fixed within specific gait phases to adjust their prosthetic knee profile. Moving forward, we aim to provide participants with a continuous knee feature space to explore while tuning their prosthetic control. Another promising avenue for reducing tuning time involves examining users' sensitivity to different control points. Understanding how changes in one control point influence the perception of others, and identifying

sensitivity levels, could inform future preference-based tuning designs, such as adjusting the number and angular resolution of control points. Successfully exploring this sensitivity could further streamline the tuning process, allowing individuals with amputations to personalize their prostheses more easily and efficiently.

In addition to the future research outlined above, our gait balance study has several limitations. First, the experiments were conducted on a treadmill at a fixed speed within a controlled lab environment. It would be beneficial to examine human responses at varying walking speeds or on level ground. Additionally, our research focused only on step width, step length, and gluteus medius (GM) activity, without measuring other biomechanical parameters such as knee and ankle kinematics and kinetics. Future research should explore additional muscle groups beyond the GM to assess whether compensatory activity occurs in other muscles. A more comprehensive analysis of human biomechanics while using our hip exoskeletons is needed to enhance our understanding.

Another important direction for future research is to establish the relationship between step width and mediolateral gait balance using key balance metrics such as whole-body angular momentum, the net external moment acting on the center of mass, and margin of stability. Developing models that directly intervene to improve the gait balance of hip exoskeleton users will also be a critical area of exploration.

BIBLIOGRAPHY

[1] C. L. McDonald, S. Westcott-Mccoy, M. R. Weaver, J. Haagsma, and D. Kartin, "Global prevalence of traumatic non-fatal limb amputation," *Prosthet. Orthot. Int.*, vol. 45, no. 2, pp. 105–114, Apr. 2021, doi: 10.1177/0309364620972258.

[2] K. Ziegler-Graham, E. J. MacKenzie, P. L. Ephraim, T. G. Travison, and R. Brookmeyer, "Estimating the Prevalence of Limb Loss in the United States: 2005 to 2050," *Arch. Phys. Med. Rehabil.*, vol. 89, no. 3, pp. 422–429, Mar. 2008, doi: 10.1016/J.APMR.2007.11.005.

[3] A. Fleming, W. Liu, and H. Huang, "Neural prosthesis control restores near-normative neuromechanics in standing postural control," *Sci. Robot.*, vol. 8, no. 83, Oct. 2023, doi: 10.1126/SCIROBOTICS.ADF5758/SUPPL_FILE/SCIROBOTICS.ADF5758_MDAR_REPRODUCIBILITY_CHECKLIST.PDF.

[4] H. M. Herr and A. M. Grabowski, "Bionic ankle–foot prosthesis normalizes walking gait for persons with leg amputation," *Proc. R. Soc. B Biol. Sci.*, vol. 279, no. 1728, p. 457, 2011, doi: 10.1098/RSPB.2011.1194.

[5] W. Liu, R. Wu, J. Si, and H. H. Huang, "A New Robotic Knee Impedance Control Parameter Optimization Method Facilitated by Inverse Reinforcement Learning," *IEEE Robot. Autom. Lett.*, vol. 7, no. 4, pp. 10882–10889, Oct. 2022, doi: 10.1109/LRA.2022.3194326.

[6] Y. Wen, J. Si, A. Brandt, X. Gao, and H. H. Huang, "Online Reinforcement Learning Control for the Personalization of a Robotic Knee Prosthesis," *IEEE Trans. Cybern.*, vol. 50, no. 6, pp. 2346–2356, Jun. 2020, doi: 10.1109/TCYB.2019.2890974.

[7] D. Quintero, D. J. Villarreal, D. J. Lambert, S. Kapp, and R. D. Gregg, "Continuous-Phase

Control of a Powered Knee-Ankle Prosthesis: Amputee Experiments Across Speeds and Inclines," *IEEE Trans. Robot.*, vol. 34, no. 3, pp. 686–701, Jun. 2018, doi: 10.1109/TRO.2018.2794536.

[8] A. Naseri, I. C. Lee, H. Huang, and M. Liu, "Investigating the Association of Quantitative Gait Stability Metrics With User Perception of Gait Interruption Due to Control Faults During Human-Prosthesis Interaction," *IEEE Trans. Neural Syst. Rehabil. Eng.*, vol. 31, pp. 4693–4702, 2023, doi: 10.1109/TNSRE.2023.3328877.

[9] T. Lenzi, M. Cempini, L. Hargrove, and T. Kuiken, "Design, development, and testing of a lightweight hybrid robotic knee prosthesis," *https://doi.org/10.1177/0278364918785993*, vol. 37, no. 8, pp. 953–976, Jul. 2018, doi: 10.1177/0278364918785993.

[10] M. Liu, F. Zhang, P. Datseris, and H. (Helen) Huang, "Improving Finite State Impedance Control of Active-Transfemoral Prosthesis Using Dempster-Shafer Based State Transition Rules," *J. Intell. Robot. Syst. Theory Appl.*, vol. 76, no. 3–4, pp. 461–474, Oct. 2014, doi: 10.1007/s10846-013-9979-3.

[11] A. F. Azocar, L. M. Mooney, J. F. Duval, A. M. Simon, L. J. Hargrove, and E. J. Rouse, "Design and clinical implementation of an open-source bionic leg," *Nat. Biomed. Eng. 2020 410*, vol. 4, no. 10, pp. 941–953, Oct. 2020, doi: 10.1038/s41551-020-00619-3.

[12] K. Kronander and A. Billard, "Stability Considerations for Variable Impedance Control," *IEEE Trans. Robot.*, vol. 32, no. 5, pp. 1298–1305, Oct. 2016, doi: 10.1109/TRO.2016.2593492.

[13] A. Alili *et al.*, "A Novel Framework to Facilitate User Preferred Tuning for a Robotic Knee Prosthesis," *IEEE Trans. Neural Syst. Rehabil. Eng.*, vol. 31, pp. 895–903, 2023, doi: 10.1109/TNSRE.2023.3236217.

[14] N. Hogan, “Adaptive control of mechanical impedance by coactivation of antagonist muscles,” *IEEE Trans. Automat. Contr.*, vol. 29, no. 8, pp. 681–690, 1984, doi: 10.1109/TAC.1984.1103644.

[15] E. Burdet, R. Osu, D. W. Franklin, T. E. Milner, and M. Kawato, “The central nervous system stabilizes unstable dynamics by learning optimal impedance,” *Nature*, vol. 414, no. 6862, pp. 446–449, Nov. 2001, doi: 10.1038/35106566.

[16] R. Gehlhar, M. Tucker, A. J. Young, and A. D. Ames, “A Review of Current State-of-the-Art Control Methods for Lower-Limb Powered Prostheses,” *Annu. Rev. Control*, vol. 55, p. 142, Jan. 2023, doi: 10.1016/J.ARCONTROL.2023.03.003.

[17] R. Baud, A. R. Manzoori, A. Ijspeert, and M. Bouri, “Review of control strategies for lower-limb exoskeletons to assist gait,” *J. NeuroEngineering Rehabil. 2021 181*, vol. 18, no. 1, pp. 1–34, Jul. 2021, doi: 10.1186/S12984-021-00906-3.

[18] K. Raab, K. Krakow, F. Tripp, and M. Jung, “Effects of training with the ReWalk exoskeleton on quality of life in incomplete spinal cord injury: a single case study,” *Spinal Cord Ser. Cases 2016 21*, vol. 2, no. 1, pp. 1–3, Jan. 2016, doi: 10.1038/scsandc.2015.25.

[19] K. A. Ingraham, M. Tucker, A. D. Ames, E. J. Rouse, and M. K. Shepherd, “Leveraging user preference in the design and evaluation of lower-limb exoskeletons and prostheses,” *Curr. Opin. Biomed. Eng.*, vol. 28, p. 100487, Dec. 2023, doi: 10.1016/J.COBME.2023.100487.

[20] J. Camargo, K. Bhakta, K. Herrin, and A. Young, “Biomechanical Evaluation of Stair Ambulation Using Impedance Control on an Active Prosthesis,” *J. Biomech. Eng.*, vol. 145, no. 2, Feb. 2023, doi: 10.1115/1.4055759/1146542.

[21] Z. F. Lerner, D. L. Damiano, H. S. Park, A. J. Gravunder, and T. C. Bulea, “A Robotic

Exoskeleton for Treatment of Crouch Gait in Children with Cerebral Palsy: Design and Initial Application," *IEEE Trans. Neural Syst. Rehabil. Eng.*, vol. 25, no. 6, pp. 650–659, Jun. 2017, doi: 10.1109/TNSRE.2016.2595501.

[22] S. Pardoel and M. Doumit, "Development and testing of a passive ankle exoskeleton," *Biocybern. Biomed. Eng.*, vol. 39, no. 3, pp. 902–913, Jul. 2019, doi: 10.1016/J.BBE.2019.08.007.

[23] S. H. Collins, M. Bruce Wiggin, and G. S. Sawicki, "Reducing the energy cost of human walking using an unpowered exoskeleton," *Nat. 2015 5227555*, vol. 522, no. 7555, pp. 212–215, Apr. 2015, doi: 10.1038/nature14288.

[24] Y. Ding, M. Kim, S. Kuindersma, and C. J. Walsh, "Human-in-the-loop optimization of hip assistance with a soft exosuit during walking," *Sci. Robot.*, vol. 3, no. 15, Feb. 2018, doi: 10.1126/SCIROBOTICS.AAR5438/SUPPL_FILE/AAR5438_SM.PDF.

[25] S. W. Hunter, F. Batchelor, K. D. Hill, A. M. Hill, S. Mackintosh, and M. Payne, "Risk Factors for Falls in People With a Lower Limb Amputation: A Systematic Review," *PM&R*, vol. 9, no. 2, pp. 170-180.e1, Feb. 2017, doi: 10.1016/J.PMRJ.2016.07.531.

[26] S. M. Felcher *et al.*, "Falls in a Young Active Amputee Population: A Frequent Cause of Rehospitalization?," *Mil. Med.*, vol. 180, no. 10, pp. 1083–1086, Oct. 2015, doi: 10.7205/MILMED-D-14-00450.

[27] F. B. Horak, "Postural orientation and equilibrium: what do we need to know about neural control of balance to prevent falls?," *Age Ageing*, vol. 35, no. suppl_2, pp. ii7–ii11, Sep. 2006, doi: 10.1093/AGEING/AFL077.

[28] C. Canbolat Seyman and Y. S. Uzar Ozcetin, "'I Wish I Could Have My Leg': A Qualitative Study on the Experiences of Individuals With Lower Limb Amputation.,"

Clin. Nurs. Res., vol. 31, no. 3, pp. 509–518, Oct. 2022, doi: 10.1177/10547738211047711.

[29] M. Goldfarb, B. E. Lawson, and A. H. Shultz, "Realizing the promise of robotic leg prostheses," *Sci. Transl. Med.*, vol. 5, no. 210, Nov. 2013, doi: 10.1126/SCITRANSLMED.3007312/ASSET/80EE60A5-FF87-4FF6-9164-F138FDCE8D07/ASSETS/GRAPHIC/5210PS15_F1.JPEG.

[30] B. E. Lawson, J. Mitchell, D. Truex, A. Shultz, E. Ledoux, and M. Goldfarb, "A robotic leg prosthesis: Design, control, and implementation," *IEEE Robot. Autom. Mag.*, vol. 21, no. 4, pp. 70–81, Dec. 2014, doi: 10.1109/MRA.2014.2360303.

[31] M. Kim and S. H. Collins, "Once-Per-Step Control of Ankle Push-Off Work Improves Balance in a Three-Dimensional Simulation of Bipedal Walking," *IEEE Trans. Robot.*, vol. 33, no. 2, pp. 406–418, Apr. 2017, doi: 10.1109/TRO.2016.2636297.

[32] Y. Sun *et al.*, "Review of Recent Progress in Robotic Knee Prosthesis Related Techniques: Structure, Actuation and Control," *J. Bionic Eng. 2021 184*, vol. 18, no. 4, pp. 764–785, Aug. 2021, doi: 10.1007/S42235-021-0065-4.

[33] A. H. Shultz and M. Goldfarb, "A Unified Controller for Walking on even and Uneven Terrain with a Powered Ankle Prosthesis," *IEEE Trans. Neural Syst. Rehabil. Eng.*, vol. 26, no. 4, pp. 788–797, Apr. 2018, doi: 10.1109/TNSRE.2018.2810165.

[34] E. P. Lamers, M. E. Eveld, and K. E. Zelik, "Subject-specific responses to an adaptive ankle prosthesis during incline walking," *J. Biomech.*, vol. 95, p. 109273, Oct. 2019, doi: 10.1016/J.JBIOMECH.2019.07.017.

[35] F. Sup, A. Bohara, and M. Goldfarb, "Design and Control of a Powered Transfemoral Prosthesis," doi: 10.1177/0278364907084588.

[36] M. Sharbafi, A. Naseri, A. Seyfarth, and M. Grimmer, “Neural control in prostheses and exoskeletons,” *Powered Prostheses Des. Control. Clin. Appl.*, pp. 153–178, Jan. 2020, doi: 10.1016/B978-0-12-817450-0.00007-9.

[37] E. M. Ficanha and M. Rastgaar, “Impedance and Admittance Controller for a Multi-Axis Powered Ankle-Foot Prosthesis,” *ASME 2014 Dyn. Syst. Control Conf. DSCC 2014*, vol. 3, Dec. 2014, doi: 10.1115/DSCC2014-6032.

[38] A. M. Simon *et al.*, “Configuring a Powered Knee and Ankle Prosthesis for Transfemoral Amputees within Five Specific Ambulation Modes,” *PLoS One*, vol. 9, no. 6, p. e99387, Jun. 2014, doi: 10.1371/journal.pone.0099387.

[39] R. Fluit, E. C. Prinsen, S. Wang, and H. Van Der Kooij, “A Comparison of Control Strategies in Commercial and Research Knee Prostheses,” *IEEE Trans. Biomed. Eng.*, vol. 67, no. 1, pp. 277–290, Jan. 2020, doi: 10.1109/TBME.2019.2912466.

[40] X. Gao, J. Si, Y. Wen, M. Li, and H. Huang, “Reinforcement Learning Control of Robotic Knee With Human-in-the-Loop by Flexible Policy Iteration,” *IEEE Trans. Neural Networks Learn. Syst.*, 2021, doi: 10.1109/TNNLS.2021.3071727.

[41] M. P. Kadaba, H. K. Ramakrishnan, and M. E. Wootten, “Measurement of lower extremity kinematics during level walking,” *J. Orthop. Res.*, vol. 8, no. 3, pp. 383–392, May 1990, doi: 10.1002/jor.1100080310.

[42] M. Li, Y. Wen, X. Gao, J. Si, and H. Huang, “Toward Expedited Impedance Tuning of a Robotic Prosthesis for Personalized Gait Assistance by Reinforcement Learning Control,” *IEEE Trans. Robot.*, 2021, doi: 10.1109/TRO.2021.3078317.

[43] S. M. H. J. Jaegers, J. H. Arendzen, and H. J. de Jongh, “Prosthetic gait of unilateral transfemoral amputees: A kinematic study,” *Arch. Phys. Med. Rehabil.*, vol. 76, no. 8, pp.

736–743, 1995, doi: 10.1016/S0003-9993(95)80528-1.

[44] B. Phillips and H. Zhao, “Predictors of Assistive Technology Abandonment,” *https://doi.org/10.1080/10400435.1993.10132205*, vol. 5, no. 1, pp. 36–45, Jun. 2010, doi: 10.1080/10400435.1993.10132205.

[45] E. Biddiss and T. Chau, “Upper-limb prosthetics: Critical factors in device abandonment,” *Am. J. Phys. Med. Rehabil.*, vol. 86, no. 12, pp. 977–987, Dec. 2007, doi: 10.1097/PHM.0B013E3181587F6C.

[46] J. Caputo *et al.*, “Robotic Emulation of Candidate Prosthetic Foot Designs May Enable Efficient, Evidence-Based, and Individualized Prescriptions,” 2021, doi: 10.1097/JPO.0000000000000409.

[47] M. K. Shepherd and E. J. Rouse, “Comparing preference of ankle–foot stiffness in below-knee amputees and prosthetists,” *Sci. Reports 2020 101*, vol. 10, no. 1, pp. 1–8, Sep. 2020, doi: 10.1038/s41598-020-72131-2.

[48] N. Thatte, H. Duan, and H. Geyer, “A Sample-Efficient Black-Box Optimizer to Train Policies for Human-in-the-Loop Systems with User Preferences,” *IEEE Robot. Autom. Lett.*, vol. 2, no. 2, pp. 993–1000, Apr. 2017, doi: 10.1109/LRA.2017.2656948.

[49] M. Tucker *et al.*, “Human preference-based learning for high-dimensional optimization of exoskeleton walking gaits,” *IEEE Int. Conf. Intell. Robot. Syst.*, pp. 3423–3430, Oct. 2020, doi: 10.1109/IROS45743.2020.9341416.

[50] R. E. Quesada, J. M. Caputo, and S. H. Collins, “Increasing ankle push-off work with a powered prosthesis does not necessarily reduce metabolic rate for transtibial amputees,” *J. Biomech.*, vol. 49, no. 14, pp. 3452–3459, Oct. 2016, doi: 10.1016/J.JBIOMECH.2016.09.015.

[51] T. R. Clites, M. K. Shepherd, K. A. Ingraham, L. Wontorcik, and E. J. Rouse, "Understanding patient preference in prosthetic ankle stiffness," *J. Neuroeng. Rehabil.*, vol. 18, no. 1, pp. 1–16, Dec. 2021, doi: 10.1186/S12984-021-00916-1/FIGURES/7.

[52] K. A. Ingraham, C. D. Remy, and E. J. Rouse, "The role of user preference in the customized control of robotic exoskeletons," *Sci. Robot.*, vol. 7, no. 64, p. 3487, Mar. 2022, doi: 10.1126/SCIROBOTICS.ABJ3487.

[53] E. G. Halsne, J. M. Czerniecki, J. B. Shofer, and D. C. Morgenroth, "The effect of prosthetic foot stiffness on foot-ankle biomechanics and relative foot stiffness perception in people with transtibial amputation," *Clin. Biomech.*, vol. 80, p. 105141, Dec. 2020, doi: 10.1016/J.CLINBIOMECH.2020.105141.

[54] M. K. Shepherd, A. F. Azocar, M. J. Major, and E. J. Rouse, "Amputee perception of prosthetic ankle stiffness during locomotion," *J. Neuroeng. Rehabil.*, vol. 15, no. 1, pp. 1–10, Nov. 2018, doi: 10.1186/S12984-018-0432-5/FIGURES/5.

[55] X. Peng, Y. Acosta-Sojo, M. I. Wu, and L. Stirling, "Actuation Timing Perception of a Powered Ankle Exoskeleton and Its Associated Ankle Angle Changes during Walking," *IEEE Trans. Neural Syst. Rehabil. Eng.*, vol. 30, pp. 869–877, 2022, doi: 10.1109/TNSRE.2022.3162213.

[56] A. Alili, V. Nalam, M. Li, M. Liu, J. Si, and H. H. Huang, "User Controlled Interface for Tuning Robotic Knee Prosthesis," *2021 IEEE/RSJ Int. Conf. Intell. Robot. Syst.*, pp. 6190–6195, Sep. 2021, doi: 10.1109/IROS51168.2021.9636264.

[57] F. Sup, H. A. Varol, J. Mitchell, T. J. Withrow, and M. Goldfarb, "Preliminary evaluations of a self-contained anthropomorphic transfemoral prosthesis," *IEEE/ASME Trans. Mechatronics*, vol. 14, no. 6, pp. 667–676, Dec. 2009, doi:

10.1109/TMECH.2009.2032688.

[58] R. Baker *et al.*, “The Conventional Gait Model - Success and Limitations,” *Handb. Hum. Motion*, vol. 1–3, pp. 489–508, Apr. 2018, doi: 10.1007/978-3-319-14418-4_25.

[59] J. B.-U. evaluation in industry and undefined 1996, “Sus: a “quick and dirty’usability,” *books.google.com*, Accessed: Mar. 14, 2022. [Online]. Available: https://books.google.com/books?hl=en&lr=&id=IfUsRmzAqvEC&oi=fnd&pg=PA189&dq=SUS+-+A+quick+and+dirty+usability+scale+John+Brooke+&ots=GbmzBeol0n&sig=_bZL9Bpep7fP4bGxeFJPBvjzeQI.

[60] R. Robinson, W. Herzog, B. N.-J. of manipulative and, and undefined 1987, “Use of force platform variables to quantify the effects of chiropractic manipulation on gait symmetry.,” *europepmc.org*, Accessed: Dec. 27, 2021. [Online]. Available: https://europepmc.org/article/med/2958572.

[61] P. Young, J. Wilken, J. D.-J. of biomechanics, and undefined 2012, “Dynamic margins of stability during human walking in destabilizing environments,” *Elsevier*, Accessed: Dec. 25, 2021. [Online]. Available: https://www.sciencedirect.com/science/article/pii/S0021929012000607?casa_token=AfpNnaUlDC4AAAAA:2S4yGrFFCLYUcVQFekq459rcpIoTnMkMFwCUnnP9JJ7zD49hJMlo8hHVTV5-dOTtoK9XP2PYXQ.

[62] R. B. Davis, S. Õunpuu, D. Tyburski, and J. R. Gage, “A gait analysis data collection and reduction technique,” *Hum. Mov. Sci.*, vol. 10, no. 5, pp. 575–587, 1991, doi: 10.1016/0167-9457(91)90046-Z.

[63] M. P. Kadaba, H. K. Ramakrishnan, M. E. Wootten, J. Gainey, G. Gorton, and G. V. B.

Cochran, “Repeatability of kinematic, kinetic, and electromyographic data in normal adult gait,” *J. Orthop. Res.*, vol. 7, no. 6, pp. 849–860, Nov. 1989, doi: 10.1002/JOR.1100070611.

[64] H. K. Ramakrishnan and M. P. Kadaba, “On the estimation of joint kinematics during gait,” *J. Biomech.*, vol. 24, no. 10, pp. 969–977, Jan. 1991, doi: 10.1016/0021-9290(91)90175-M.

[65] A. L. Hof, M. G. J. Gazendam, and W. E. Sinke, “The condition for dynamic stability,” *J. Biomech.*, vol. 38, pp. 1–8, 2005, doi: 10.1016/j.jbiomech.2004.03.025.

[66] A. L. Hof, R. M. van Bockel, T. Schoppen, and K. Postema, “Control of lateral balance in walking: Experimental findings in normal subjects and above-knee amputees,” *Gait Posture*, vol. 25, no. 2, pp. 250–258, Feb. 2007, doi: 10.1016/J.GAITPOST.2006.04.013.

[67] J. Yuan, X. Bai, A. Alili, M. Liu, J. Feng, and H. Huang, “Understanding the Preferences for Lower-Limb Prosthesis: A Think-Aloud Study during User-Guided Auto-Tuning,” *https://doi.org/10.1177/1071181322661082*, vol. 66, no. 1, pp. 2159–2163, Oct. 2022, doi: 10.1177/1071181322661082.

[68] J. Yuan, X. Bai, A. Alili, M. Liu, J. Feng, and H. Huang, “Finding a Natural Fit: A Thematic Analysis of Amputees’ Prosthesis Setting Preferences during User-Guided Auto-Tuning,” *https://doi.org/10.1177/21695067231216121*, vol. 67, no. 1, pp. 2591–2597, Nov. 2023, doi: 10.1177/21695067231216121.

[69] R. Gailey, K. Allen, J. Castles, J. Kucharik, and M. Roeder, “Review of secondary physical conditions associated with lower-limb amputation and long-term prosthesis use,” vol. 45, no. 1, 2008, doi: 10.1682/JRRD.2006.11.0147.

[70] A. Brandt, W. Riddick, J. Stallrich, M. Lewek, and H. H. Huang, “Effects of extended

powered knee prosthesis stance time via visual feedback on gait symmetry of individuals with unilateral amputation: A preliminary study," *J. Neuroeng. Rehabil.*, vol. 16, no. 1, pp. 1–12, Sep. 2019, doi: 10.1186/S12984-019-0583-Z/FIGURES/4.

[71] F. Zhang, M. Liu, and H. Huang, "Effects of locomotion mode recognition errors on volitional control of powered above-knee prostheses," *IEEE Trans. Neural Syst. Rehabil. Eng.*, vol. 23, no. 1, pp. 64–72, Jan. 2015, doi: 10.1109/TNSRE.2014.2327230.

[72] Y. Wang and M. Srinivasan, "Stepping in the direction of the fall: the next foot placement can be predicted from current upper body state in steady-state walking," *Biol. Lett.*, vol. 10, no. 9, Sep. 2014, doi: 10.1098/RSBL.2014.0405.

[73] P.-F. T. Marjorie H Woollacot, "Balance Control During Walking in the Older Adult: Research and Its Implications," Accessed: Dec. 15, 2022. [Online]. Available: https://academic.oup.com/ptj/article/77/6/646/2633159.

[74] T. Mcgeer, "Passive Dynamic Walking," *Int. J. Rob. Res.*, vol. 9, no. 2, pp. 62–82, 1990, doi: 10.1177/027836499000900206.

[75] A. D. Kuo, "Stabilization of lateral motion in passive dynamic walking," *Int. J. Rob. Res.*, vol. 18, no. 9, pp. 917–930, 1999, doi: 10.1177/02783649922066655.

[76] T. Lencioni *et al.*, "Strategies for maintaining dynamic balance in persons with neurological disorders during overground walking," *J Eng. Med.*, vol. 235, no. 9, pp. 1079–1087, 2021, doi: 10.1177/09544119211023624.

[77] S. Morrison, C. A. Rynders, and J. J. Sosnoff, "Deficits in medio-lateral balance control and the implications for falls in individuals with multiple sclerosis," *Gait Posture*, vol. 49, pp. 148–154, Sep. 2016, doi: 10.1016/J.GAITPOST.2016.06.036.

[78] B. Sidaway *et al.*, "The identification of fall risk through tests of mediolateral stability

during gait," *Exp. Gerontol.*, vol. 163, Jun. 2022, doi: 10.1016/J.EXGER.2022.111803.

[79] B. M. Shin, S. J. Han, J. H. Jung, J. E. Kim, and F. Fregni, "Effect of mild cognitive impairment on balance," *J. Neurol. Sci.*, vol. 305, no. 1–2, pp. 121–125, Jun. 2011, doi: 10.1016/J.JNS.2011.02.031.

[80] H. Reimann, T. Fettrow, and J. J. Jeka, "Strategies for the Control of Balance During Locomotion," *Kinesiol. Rev.*, vol. 7, no. 1, pp. 18–25, Feb. 2018, doi: 10.1123/KR.2017-0053.

[81] C. E. Bauby and A. D. Kuo, "Active control of lateral balance in human walking," *J. Biomech.*, vol. 33, no. 11, pp. 1433–1440, Nov. 2000, doi: 10.1016/S0021-9290(00)00101-9.

[82] B. L. Rankin, S. K. Buffo, and J. C. Dean, "A neuromechanical strategy for mediolateral foot placement in walking humans," *J. Neurophysiol.*, vol. 112, no. 2, pp. 374–383, 2014, doi: 10.1152/jn.00138.2014.

[83] D. J. Farris and G. S. Sawicki, "The mechanics and energetics of human walking and running: a joint level perspective," *J. R. Soc. Interface*, vol. 9, no. 66, pp. 110–118, Jan. 2012, doi: 10.1098/RSIF.2011.0182.

[84] S. A. Roelker, S. A. Kautz, and R. R. Neptune, "Muscle contributions to mediolateral and anteroposterior foot placement during walking," *J. Biomech.*, vol. 95, Oct. 2019, doi: 10.1016/J.JBIOMECH.2019.08.004.

[85] J. C. Dean, N. B. Alexander, and A. D. Kuo, "The effect of lateral stabilization on walking in young and old adults," *IEEE Trans. Biomed. Eng.*, vol. 54, no. 11, pp. 1919–1926, Nov. 2007, doi: 10.1109/TBME.2007.901031.

[86] T. Caderby, E. Yiou, N. Peyrot, M. Begon, and G. Dalleau, "Influence of gait speed on the

control of mediolateral dynamic stability during gait initiation," *J. Biomech.*, vol. 47, no. 2, pp. 417–423, Jan. 2014, doi: 10.1016/J.JBIOMECH.2013.11.011.

[87] M. Mancini and F. B. Horak, "The relevance of clinical balance assessment tools to differentiate balance deficits," *Eur. J. Phys. Rehabil. Med.*, vol. 46, no. 2, p. 239, Jun. 2010, Accessed: Oct. 05, 2024. [Online]. Available: /pmc/articles/PMC3033730/.

[88] L. Hak, H. Houdijk, P. J. Beek, J. H. Van Dieë, and A. A. Zadpoor, "Steps to Take to Enhance Gait Stability: The Effect of Stride Frequency, Stride Length, and Walking Speed on Local Dynamic Stability and Margins of Stability," 2013, doi: 10.1371/journal.pone.0082842.

[89] A. L. Hof, R. M. van Bockel, T. Schoppen, and K. Postema, "Control of lateral balance in walking: Experimental findings in normal subjects and above-knee amputees," *Gait Posture*, vol. 25, no. 2, pp. 250–258, Feb. 2007, doi: 10.1016/J.GAITPOST.2006.04.013.

[90] M. Roerdink, C. J. C. Lamoth, G. Kwakkel, P. C. W. Van Wieringen, and P. J. Beek, "Gait Coordination After Stroke: Benefits of Acoustically Paced Treadmill Walking," *Phys. Ther.*, vol. 87, no. 8, pp. 1009–1022, Aug. 2007, doi: 10.2522/PTJ.20050394.

[91] M. D. Lewek, C. E. Bradley, C. J. Wutzke, and S. M. Zinder, "The Relationship Between Spatiotemporal Gait Asymmetry and Balance in Individuals With Chronic Stroke," *J. Appl. Biomech.*, vol. 30, no. 1, pp. 31–36, Feb. 2014, doi: 10.1123/JAB.2012-0208.

[92] N. K. Reimold, H. A. Knapp, A. N. Chesnutt, A. Agne, and J. C. Dean, "Effects of Targeted Assistance and Perturbations on the Relationship between Pelvis Motion and Step Width in People with Chronic Stroke," *IEEE Trans. Neural Syst. Rehabil. Eng.*, vol. 29, pp. 134–143, 2021, doi: 10.1109/TNSRE.2020.3038173.

[93] J. M. Donelan, D. W. Shipman, R. Kram, and A. D. Kuo, "Mechanical and metabolic

requirements for active lateral stabilization in human walking," *J. Biomech.*, vol. 37, no. 6, pp. 827–835, Jun. 2004, doi: 10.1016/J.JBIOMECH.2003.06.002.

[94] M. M. Wu, G. L. Brown, J. L. Woodward, S. M. Bruijn, and K. E. Gordon, "A novel Movement Amplification environment reveals effects of controlling lateral centre of mass motion on gait stability and metabolic cost," *R. Soc. Open Sci.*, vol. 7, no. 1, Jan. 2020, doi: 10.1098/RSOS.190889.

[95] J. F. Veneman, J. Menger, E. H. F. van Asseldonk, F. C. T. van der Helm, and H. van der Kooij, "Fixating the pelvis in the horizontal plane affects gait characteristics," *Gait Posture*, vol. 28, no. 1, pp. 157–163, Jul. 2008, doi: 10.1016/J.GAITPOST.2007.11.008.

[96] A. Pennycott, D. Wyss, H. Vallery, and R. Riener, "Effects of added inertia and body weight support on lateral balance control during walking," *IEEE Int. Conf. Rehabil. Robot.*, 2011, doi: 10.1109/ICORR.2011.5975415.

[97] L. N. Heitkamp, K. H. Stimpson, and J. C. Dean, "Application of a Novel Force-Field to Manipulate the Relationship between Pelvis Motion and Step Width in Human Walking," *IEEE Trans. Neural Syst. Rehabil. Eng.*, vol. 27, no. 10, pp. 2051–2058, Oct. 2019, doi: 10.1109/TNSRE.2019.2941372.

[98] M. F. Hamza, R. A. R. Ghazilla, B. B. Muhammad, and H. J. Yap, "Balance and stability issues in lower extremity exoskeletons: A systematic review," *Biocybern. Biomed. Eng.*, vol. 40, no. 4, pp. 1666–1679, 2020, doi: 10.1016/j.bbe.2020.09.004.

[99] V. Monaco *et al.*, "An ecologically-controlled exoskeleton can improve balance recovery after slippage," *Sci. Reports 2017 71*, vol. 7, no. 1, pp. 1–10, May 2017, doi: 10.1038/srep46721.

[100] S. Qiu *et al.*, "A Unified Active Assistance Control Framework of Hip Exoskeleton for

Walking and Balance Assistance∗," *IEEE Int. Conf. Intell. Robot. Syst.*, pp. 8185–8192, Nov. 2019, doi: 10.1109/IROS40897.2019.8968055.

[101] T. Zhang, M. Tran, and H. Huang, "Design and experimental verification of hip exoskeleton with balance capacities for walking assistance," *IEEE/ASME Trans. Mechatronics*, vol. 23, no. 1, pp. 274–285, Feb. 2018, doi: 10.1109/TMECH.2018.2790358.

[102] T. Zhang, M. Tran, and H. Huang, "Admittance shaping-based assistive control of SEA-driven robotic hip exoskeleton," *IEEE/ASME Trans. Mechatronics*, vol. 24, no. 4, pp. 1508–1519, Aug. 2020, doi: 10.1109/TMECH.2019.2916546.

[103] V. L. Chiu, M. Raitor, and S. H. Collins, "Design of a Hip Exoskeleton With Actuation in Frontal and Sagittal Planes," *IEEE Trans. Med. Robot. Bionics*, vol. 3, no. 3, pp. 773–782, Aug. 2021, doi: 10.1109/TMRB.2021.3088521.

[104] V. Nalam, A. Alili, A. Fleming, X. Tu, M. Liu, and H. Huang, "Development of a Hip Abduction-Adduction Exoskeleton for Mediolateral Assistance," *Authorea Prepr.*, Mar. 2024, doi: 10.36227/TECHRXIV.171171958.81255425/V1.

[105] F. Caccavale, C. Natale, B. Siciliano, and L. Villani, "Integration for the next generation: Embedding force control into industrial robots," *IEEE Robot. Autom. Mag.*, vol. 12, no. 3, pp. 53–64, Sep. 2005, doi: 10.1109/MRA.2005.1511869.

[106] B. J. Darter, E. D. Syrett, K. B. Foreman, E. Kubiak, and S. Sinclair, "Changes in frontal plane kinematics over 12-months in individuals with the Percutaneous Osseointegrated Prosthesis (POP)," *PLoS One*, vol. 18, no. 2, p. e0281339, Feb. 2023, doi: 10.1371/JOURNAL.PONE.0281339.

[107] S. N. Kubinski, C. A. McQueen, K. A. Sittloh, and J. C. Dean, "Walking with wider steps

increases stance phase gluteus medius activity," *Gait Posture*, vol. 41, no. 1, pp. 130–135, Jan. 2015, doi: 10.1016/J.GAITPOST.2014.09.013.

[108] M. Afschrift, L. Pitto, W. Aerts, R. Van Deursen, I. Jonkers, and F. De Groote, "Modulation of gluteus medius activity reflects the potential of the muscle to meet the mechanical demands during perturbed walking OPEN," *Sci. REPORts* |, vol. 8, p. 11675, 2018, doi: 10.1038/s41598-018-30139-9.

[109] H. J. Hermens *et al.*, "European Recommendations for Surface ElectroMyoGraphy Results of the SENIAM project."

[110] J. L. Helbostad and R. Moe-Nilssen, "The effect of gait speed on lateral balance control during walking in healthy elderly," *Gait Posture*, vol. 18, no. 2, pp. 27–36, Oct. 2003, doi: 10.1016/S0966-6362(02)00197-2.

[111] C. Karakasis and P. Artemiadis, "F-VESPA: A Kinematic-based Algorithm for Real-time Heel-strike Detection during Walking," *IEEE Int. Conf. Intell. Robot. Syst.*, pp. 5098–5103, 2021, doi: 10.1109/IROS51168.2021.9636335.

[112] G. E. P. Box, G. M. Jenkins, G. C. Reinsel, and G. M. Ljung, *Time series analysis: forecasting and control*. John Wiley \& Sons, 2015.

[113] T. P. Luu *et al.*, "Multi-trial gait adaptation of healthy individuals during visual kinematic perturbations," *Front. Hum. Neurosci.*, vol. 11, p. 320, Jun. 2017, doi: 10.3389/FNHUM.2017.00320/BIBTEX.

[114] J. F. Yang and D. A. Winter, "Electromyographic amplitude normalization methods: improving their sensitivity as diagnostic tools in gait analysis.," *Arch. Phys. Med. Rehabil.*, vol. 65, no. 9, pp. 517–521, Sep. 1984, Accessed: Dec. 23, 2022. [Online]. Available: https://europepmc.org/article/med/6477083.

[115] A. L. Hof, H. Elzinga, W. Grimmius, and J. P. K. Halbertsma, “Speed dependence of averaged EMG profiles in walking,” *Gait Posture*, vol. 16, no. 1, pp. 78–86, Aug. 2002, doi: 10.1016/S0966-6362(01)00206-5.

[116] X. Tu, M. Li, M. Liu, J. Si, and H. Huang, “A Data-Driven Reinforcement Learning Solution Framework for Optimal and Adaptive Personalization of a Hip Exoskeleton,” *Proc. - IEEE Int. Conf. Robot. Autom.*, vol. 2021-May, pp. 10610–10616, 2021, doi: 10.1109/ICRA48506.2021.9562062.

[117] T. Lenzi, S. M. M. De Rossi, N. Vitiello, and M. C. Carrozza, “Intention-based EMG control for powered exoskeletons,” *IEEE Trans. Biomed. Eng.*, vol. 59, no. 8, pp. 2180–2190, 2012, doi: 10.1109/TBME.2012.2198821.

[118] V. Nalam, X. Tu, M. Li, J. Si, and H. H. Huang, “Admittance Control Based Human-in-the-Loop Optimization for Hip Exoskeleton Reduces Human Exertion during Walking,” *Proc. - IEEE Int. Conf. Robot. Autom.*, pp. 6743–6749, 2022, doi: 10.1109/ICRA46639.2022.9811553.

[119] A. Martinez, B. Lawson, C. Durrough, and M. Goldfarb, “A Velocity-Field-Based Controller for Assisting Leg Movement during Walking with a Bilateral Hip and Knee Lower Limb Exoskeleton,” *IEEE Trans. Robot.*, vol. 35, no. 2, pp. 307–316, Apr. 2019, doi: 10.1109/TRO.2018.2883819.

[120] A. Alili, V. Nalam, A. Fleming, M. Liu, J. Dean, and H. He Huang, “Closed-Loop Feedback Control of Human Step Width During Walking by Mediolaterally Acting Robotic Hip Exoskeleton,” pp. 6097–6102, Dec. 2023, doi: 10.1109/IROS55552.2023.10342127.

[121] J. C. Dean, A. E. Embry, K. H. Stimpson, L. A. Perry, and S. A. Kautz, “Effects of hip

abduction and adduction accuracy on post-stroke gait," *Clin. Biomech.*, vol. 44, pp. 14–20, May 2017, doi: 10.1016/J.CLINBIOMECH.2017.02.013.

[122] T. Burton, E. Seguin, and M. Doumit, "Study of Hip Exoskeleton Technology for Elderly Stability During Walking," *2022 World Autom. Congr.*, pp. 596–601, Oct. 2022, doi: 10.23919/WAC55640.2022.9934512.

[123] A. Brandt and H. (Helen) Huang, "Effects of extended stance time on a powered knee prosthesis and gait symmetry on the lateral control of balance during walking in individuals with unilateral amputation," *J. Neuroeng. Rehabil.*, vol. 16, no. 1, pp. 1–11, Nov. 2019, doi: 10.1186/S12984-019-0625-6/FIGURES/3.

[124] V. Nalam and H. (Helen) Huang, "Empowering prosthesis users with a hip exoskeleton," *Nat. Med. 2021 2710*, vol. 27, no. 10, pp. 1677–1678, Oct. 2021, doi: 10.1038/s41591-021-01529-w.

[125] A. D. Kuo and J. M. Donelan, "Dynamic Principles of Gait and Their Clinical Implications," *Phys. Ther.*, vol. 90, no. 2, pp. 157–174, Feb. 2010, doi: 10.2522/PTJ.20090125.

[126] R. Baud, A. R. Manzoori, A. Ijspeert, and M. Bouri, "Review of control strategies for lower-limb exoskeletons to assist gait," *J. NeuroEngineering Rehabil. 2021 181*, vol. 18, no. 1, pp. 1–34, Jul. 2021, doi: 10.1186/S12984-021-00906-3.

[127] Y. Chen, G. Chen, J. Ye, C. Fu, B. Liang, and X. Li, "Learning to Assist Different Wearers in Multitasks: Efficient and Individualized Human-In-the-Loop Adaption Framework for Exoskeleton Robots," Sep. 2023, doi: 10.1109/TRO.2024.3468768.

[128] A. D. Kuo, "Stabilization of lateral motion in passive dynamic walking," *Int. J. Rob. Res.*, vol. 18, no. 9, pp. 917–930, 1999, doi: 10.1177/02783649922066655.

[129] S. M. O'Connor and A. D. Kuo, "Direction-dependent control of balance during walking and standing," *J. Neurophysiol.*, vol. 102, no. 3, pp. 1411–1419, Sep. 2009, doi: 10.1152/JN.00131.2009/ASSET/IMAGES/LARGE/Z9K0090996470006.JPEG.

[130] M. Arvin, J. H. van Dieën, and S. M. Bruijn, "Effects of constrained trunk movement on frontal plane gait kinematics," *J. Biomech.*, vol. 49, no. 13, pp. 3085–3089, Sep. 2016, doi: 10.1016/J.JBIOMECH.2016.07.015.

[131] C. E. Bauby and A. D. Kuo, "Active control of lateral balance in human walking," *J. Biomech.*, vol. 33, no. 11, pp. 1433–1440, 2000, doi: 10.1016/S0021-9290(00)00101-9.

[132] L. K. Molina, G. H. Small, and R. R. Neptune, "The influence of step width on balance control and response strategies during perturbed walking in healthy young adults," *J. Biomech.*, vol. 157, p. 111731, Aug. 2023, doi: 10.1016/J.JBIOMECH.2023.111731.

[133] S. A. Roelker, S. A. Kautz, and R. R. Neptune, "Muscle contributions to mediolateral and anteroposterior foot placement during walking," *J. Biomech.*, vol. 95, p. 109310, Oct. 2019, doi: 10.1016/J.JBIOMECH.2019.08.004.

[134] S. Wang *et al.*, "Design and Control of the MINDWALKER Exoskeleton," *IEEE Trans. Neural Syst. Rehabil. Eng.*, vol. 23, no. 2, pp. 277–286, 2015, doi: 10.1109/TNSRE.2014.2365697.

[135] V. L. Chiu, M. Raitor, and S. H. Collins, "Design of a Hip Exoskeleton With Actuation in Frontal and Sagittal Planes," *IEEE Trans. Med. Robot. Bionics*, vol. 3, no. 3, pp. 773–782, Jun. 2021, doi: 10.1109/TMRB.2021.3088521.

[136] J. K. Leestma, S. Mathur, M. D. Anderton, G. S. Sawicki, and A. J. Young, "Dynamic Duo: Design and Validation of an Autonomous Frontal and Sagittal Actuating Hip Exoskeleton for Balance Modulation during Perturbed Locomotion," *IEEE Robot. Autom.*

Lett., vol. 9, no. 5, pp. 3995–4002, May 2024, doi: 10.1109/LRA.2024.3371290.

[137] V. Nalam, A. Alili, A. Fleming, X. Tu, M. Liu, and H. Huang, "Development of a Hip Abduction-Adduction Exoskeleton for Mediolateral Assistance," *Authorea Prepr.*, Mar. 2024, doi: 10.36227/TECHRXIV.171171958.81255425/V1.

[138] D. P. Henson *et al.*, "Understanding lower limb muscle volume adaptations to amputation," *J. Biomech.*, vol. 125, p. 110599, Aug. 2021, doi: 10.1016/J.JBIOMECH.2021.110599.

[139] S. Dorsch, L. Ada, and C. G. Canning, "Lower Limb Strength Is Significantly Impaired in All Muscle Groups in Ambulatory People With Chronic Stroke: A Cross-Sectional Study," *Arch. Phys. Med. Rehabil.*, vol. 97, no. 4, pp. 522–527, Apr. 2016, doi: 10.1016/J.APMR.2015.10.106.

[140] A. Sawers and S. Fatone, "The relationship of hip strength to walking and balance performance in unilateral lower limb prosthesis users differs by amputation level," *PM&R*, 2024, doi: 10.1002/PMRJ.13245.

[141] S. L. Molitor and R. R. Neptune, "Lower-limb joint quasi-stiffness in the frontal and sagittal planes during walking at different step widths," *J. Biomech.*, vol. 162, p. 111897, Jan. 2024, doi: 10.1016/J.JBIOMECH.2023.111897.

[142] A. Alili, V. Nalam, A. Fleming, M. Liu, J. Dean, and H. He Huang, "Closed-Loop Feedback Control of Human Step Width During Walking by Mediolaterally Acting Robotic Hip Exoskeleton," *IEEE Int. Conf. Intell. Robot. Syst.*, pp. 6097–6102, 2023, doi: 10.1109/IROS55552.2023.10342127.

[143] A. Alili, A. Fleming, V. Nalam, M. Liu, J. Dean, and H. Huang, "Abduction/Adduction Assistance From Powered Hip Exoskeleton Enables Modulation of User Step Width

During Walking," *IEEE Trans. Biomed. Eng.*, vol. 71, no. 1, pp. 334–342, Jan. 2024, doi: 10.1109/TBME.2023.3301444.

[144] J. Lee, H. R. Warren, V. Agarwal, M. E. Huber, and N. Hogan, "Modulating hip stiffness with a robotic exoskeleton immediately changes gait," *Proc. - IEEE Int. Conf. Robot. Autom.*, pp. 733–739, 2020, doi: 10.1109/ICRA40945.2020.9197054.

[145] T. Lillicrap *et al.*, "Continuous control with deep reinforcement learning," *Int. Conf. Learn. Represent.*, 2015.

[146] J. L. Helbostad and R. Moe-Nilssen, "The effect of gait speed on lateral balance control during walking in healthy elderly," *Gait Posture*, vol. 18, no. 2, pp. 27–36, Oct. 2003, doi: 10.1016/S0966-6362(02)00197-2.

[147] M. Mangalam, A. Skiadopoulos, K. C. Siu, M. Mukherjee, A. Likens, and N. Stergiou, "Leveraging a virtual alley with continuously varying width modulates step width variability during self-paced treadmill walking," *Neurosci. Lett.*, vol. 793, p. 136966, Jan. 2023, doi: 10.1016/J.NEULET.2022.136966.

[148] T. M. Owings and M. D. Grabiner, "Step width variability, but not step length variability or step time variability, discriminates gait of healthy young and older adults during treadmill locomotion," *J. Biomech.*, vol. 37, no. 6, pp. 935–938, Jun. 2004, doi: 10.1016/J.JBIOMECH.2003.11.012.

[149] M. A. Diaz *et al.*, "Human-in-the-Loop Optimization of Wearable Robotic Devices to Improve Human-Robot Interaction: A Systematic Review," *IEEE Trans. Cybern.*, vol. 53, no. 12, pp. 7483–7496, Dec. 2023, doi: 10.1109/TCYB.2022.3224895.

[150] J. R. T. and H. (Helen) H. Abbas Alili, Varun Nalam, "Exploring the Impact of Continuous Mediolateral Torque Application by Hip Exoskeleton on the Gait Balance of

Non-Disabled Individuals," *46th Annu. Int. Conf. IEEE Eng. Med. Biol. Soc.*, 2024.

[151] M. H. G. Gerards *et al.*, "Adaptability to Balance Perturbations During Walking as a Potential Marker of Falls History in Older Adults," *Front. Sport. Act. Living*, vol. 0, p. 132, May 2021, doi: 10.3389/FSPOR.2021.682861.

[152] S. Shokouhi, P. Sritharan, & Peter, and V.-S. Lee, "Recovering whole-body angular momentum and margin of stability after treadmill-induced perturbations during sloped walking in healthy young adults," *Sci. Reports* |, vol. 14, p. 4421, 123AD, doi: 10.1038/s41598-024-54890-4.

[153] A. Skiadopoulos, E. E. Moore, H. R. Sayles, K. K. Schmid, and N. Stergiou, "Step width variability as a discriminator of age-related gait changes," *J. Neuroeng. Rehabil.*, vol. 17, no. 1, pp. 1–13, Mar. 2020, doi: 10.1186/S12984-020-00671-9/FIGURES/4.

[154] C. B. Sanz-Morère *et al.*, "Robot-mediated overground gait training for transfemoral amputees with a powered bilateral hip orthosis: a pilot study," *J. Neuroeng. Rehabil.*, vol. 18, no. 1, pp. 1–17, Dec. 2021, doi: 10.1186/S12984-021-00902-7/FIGURES/4.

[155] S.-H. Lee, J. Kim, B. Lim, H.-J. Lee, and Y.-H. Kim, "Exercise with a wearable hip-assist robot improved physical function and walking efficiency in older adults," 123AD, doi: 10.1038/s41598-023-32335-8.

[156] A. A. Krause *et al.*, "Effect of mediolateral leg perturbations on walking balance in people with chronic stroke: A randomized controlled trial," *PLoS One*, vol. 19, no. 10, p. e0311727, 2024, doi: 10.1371/JOURNAL.PONE.0311727.

[157] A. M. van Leeuwen, S. M. Bruijn, and J. C. Dean, "Force-field perturbations and muscle vibration strengthen stability-related foot placement responses during steady-state gait in healthy adults," *Hum. Mov. Sci.*, vol. 96, p. 103243, Aug. 2024, doi:

10.1016/J.HUMOV.2024.103243.

APPENDICES

Appendix A

The CUSUM algorithm is used to detect small incremental changes in the mean of a process. Given a sequence $s_1, s_2, s_3, \ldots, s_n$ with target average m_s and target standard deviation σ_s, upper (U_i) and lower (L_i) cumulative process sums are defined as:

$$U_i = \begin{cases} 0, & i = 1 \\ \max\left(0,\ U_{i-1} + s_i - m_s - \frac{1}{2}n\sigma_s\right), & i > 1 \end{cases}$$

$$L_i = \begin{cases} 0, & i = 1 \\ min\left(0,\ L_{i-1} + s_i - m_s + \frac{1}{2}n\sigma_s\right), & i > 1 \end{cases}$$

The variable n is the number of standard deviations from the target mean that makes a shift of mean detectable. A process violates the CUSUM criterion at the sample s_j if it obeys $U_j > c\sigma_s$ or $L_j < -c\sigma_s$.

In this study, we defined the sequence as the set of step width measurements taken before the *K* changed (i.e., the 20 consecutive heel strikes leading up to the change), merged with all the step width data corresponding to a new *K* value. We defined the mean and standard deviation of the step width data samples taken before the *K* change as m_s and σ_s. To set the control limit c for the subsequent analysis, we chose a value of 3, and set n to 1.